# Measuring the intrinsic kinetics of heterogeneously catalyzed reactions in gas-solid bubbling fluidized beds: criteria and case study

Juray DE WILDE

Université catholique de Louvain (UCLouvain), Materials and Process Engineering (IMAP),

Place Sainte Barbe 2, B-1348 Louvain-la-Neuve, Belgium,

Tel.: +32 10 47 8193, Fax: +32 10 47 4028, e-mail: juray.dewilde@uclouvain.be

**Abstract**

The paper presents a set of criteria that has to be satisfied in order to ensure that the intrinsic kinetics of heterogeneously catalyzed reactions is measured with a certain precision in a gas-solid bubbling fluidized bed. Bubbling fluidization has to be ensured while slugging and channelling have to be avoided and the pressure drop over the bed has to be sufficiently small. To allow using an ideal-flow pattern reactor model for the estimation of the rate parameters, the influence of axial dispersion has to be verified. For the bubble phase, negligeable axial dispersion is aimed at, whereas for the emulsion phase gas two ideal situations can be considered, negligeable axial dispersion or dominant axial dispersion. For reacting particles in the emulsion phase, the assumption of complete mixing is to be evaluated. Isothermal operation is essential to extract intrinsic reaction kinetics from the conversion versus space time data and requires a negligeable radial temperature gradient. Bed dilution can be applied to ensure isothermal operation, but segregation needs to be avoided. Various interfacial transfer and intra-particle transport limitations have to be negligible. For negligible gas-solid heat and mass transfer limitations and for negligible intra-particle heat and species transport limitations, criteria developed for fixed bed reactors can be adopted. A similar criterion for negligible bubble-emulsion phase mass transfer limitations is presented. Following the theoretical analysis, a case study illustrates the main challenges in measuring intrinsic reaction kinetics.

## 1. INTRODUCTION

Fluidized bed reactors have gained attention for studying intrinsic reaction kinetics as an alternative for packed bed reactors because of their excellent temperature uniformity resulting from intense mixing of particles in the bed [Kunii & Levenspiel, 1991]. Another advantage is that particles can be fed to or removed from the bed, which can be of interest when the particles take part in the reaction and taking a particle sample can give valuable information about the reaction mechanism and kinetics. Furthermore, it may be desirable to determine the reaction kinetics with the fluidizable catalyst particles themselves, rather than with a pelletized form. So-called Micro-Fluidized Beds (MFB) with a typical diameter (ID) in the range 15-30 mm are used to prevent excessive gas consumption while allowing fluidization of the bed.

Depending on the type of particles used and the (superficial) velocity of the fluidizing gas, various fluidization regimes exist [Geldart, 1973], from the smoothly expanded aerated bed regime at low velocities, via the bubbling and turbulent fluidized bed, to the fast fluidized bed regime and the pneumatic transport or riser type regime at high velocities [Kunii & Levenspiel, 1991]. These regimes have distinctly different flow behaviours and require specific correlations for calculating the transport properties of the bed. For measuring reaction kinetics, transport or riser type reactors are not frequently used as they are typically adiabatically operated and isothermal operation cannot be ensured. Furthermore, gas and particles have to be efficiently mixed at the reactor inlet and separated at the reactor outlet to ensure a known and uniform gas-solids contact time. Therefore, this paper focuses on the typically used bubbling fluidized bed regime.

For packed bed reactors, an ensemble of criteria was developed to verify to what extent intrinsic reaction kinetics can be extracted from conversion versus space time data [Froment et al., 2010]. These essentially verify that the reaction conditions that have to be related to the observed reaction rates are known with sufficient accuracy. Meeting the criteria also allows simplifying the reactor model to be used in the parameter estimation and a computationally tractable regression.

The criteria have been applied in various studies [e.g. De Wilde et al., 2001; Minette et al., 2018]. Meeting all of the criteria is typically only possible in a limited window of operating conditions. A limited temperature window is particularly problematic as this affects the precision of the estimation of the activation energies and heats of adsorption. Isothermal operation is essential to facilitate kinetic modelling. The use of a fluidized bed reactor then seems an attractive option, but despite intense mixing in the particle bed, temperature uniformity is not necessarily guaranteed. Furthermore, when using a fluidized bed, other criteria may be more difficult to meet. For example, interfacial transfer limitations may be difficult to eliminate because of the limited slip velocity between gas and particles that cannot exceed the terminal velocity of the particles in the earth gravitational field. Totally avoiding particle entrainment may also be challenging. Capturing and recirculating entrained particles is in principle possible, but may complicate the data analysis, e.g. in case of segregation of inert and catalyst particles or in case the particles participate in the reaction. Finally, phenomena that do not exist in a packed bed have to be dealt with [Kunii and Levenspiel, 1991; Froment et al., 2010] and their importance in falsifying measurements of intrinsic reaction kinetics evaluated through specific criteria that are derived in this paper: criteria ensuring bubbling fluidization and avoidance of large-scale non-uniformities in the bed, such as slugging and channelling; criteria allowing idealization of axial dispersion of the gas introduced by the mixing of the particle bed; modified criteria for isothermal operation; criteria to evaluate bubble-emulsion phase mass transfer limitations and related gas bypassing; and criteria to evaluate eventual segregation between catalyst and diluent particles. These new criteria are to be combined with existing criteria for interfacial gas-solid mass and heat transfer and intra-particle mass and heat transport. An overview of the different aspects to be dealt with when aiming at observing intrinsic reactions kinetics in a bubbling fluidized bed is shown in Figure 1.

Although a number of kinetic studies using a fluidized bed experimentally verified the absence of interfacial mass and heat transfer limitations, the absence of intra-particle diffusion limitations and isothermal operation [Beyke, 1986; Chen et al., 2015, 2017, 2017b; Gao et al., 2017; Li

et al., 2020], only few papers present an incomplete theoretical verification [Guo et al., 2016, 2016b; Zhang et al., 2014, 2015, 2015b]. This paper therefore focuses on the development of a complete set of criteria to verify to what extent intrinsic reaction kinetics can be extracted from measurements with a bubbling fluidized bed reactor, focusing on gas-solid fluidized beds and catalytic reactions. Example correlations for the various transport properties that need to be calculated are given. It is, however, out of the scope of this paper to present a complete review of all such published correlations. A case study is presented at the end of the paper to illustrate the main challenge for measuring intrinsic reaction kinetics. The paper focuses on gas-solid fluidized beds, but the presented approach can be easily adapted to gas-liquid or three-phase flow operation using the appropriate correlations for the transport properties.

## 2. FLOW PATTERN AND PRESSURE DROP

In a fixed bed reactor, plug flow is typically aimed at for the gas phase. Radially uniform velocity and temperature profiles require turbulent flow and, hence, a sufficiently high particle Reynolds number, typically $Re_p = \rho_g u_s d_p/\mu > 10 - 20$ [Carberry, 1963; 1976] depending on whether plug flow or fully turbulent flow is aimed at. In fluidized bed reactors, such particle Reynolds numbers can typically not be achieved, at the lab and even industrial scale, because the gas-solids slip velocity is limited to the terminal velocity of the particles. In a fluidized bed, radial mixing is, however, not only the result of turbulence in the gas phase, but also of the lateral motion of the particles and bubbles. Hence, radially uniformity can be achieved at lower Reynolds numbers and criteria focus on ensuring a bubbling fluidized bed state.

### 2.1. Bubbling fluidization

The pressure drop or gas velocity needs to be sufficiently high for the bed to be fluidized and bubbling without causing significant entrainment of particles from the bed. Quasi-isobaric operation

also requires the hydrostatic pressure drop over the bed to be sufficiently small. For the bed to be fluidized, the superficial velocity of the fluidizing gas has to exceed the minimum fluidization velocity:

$$u_{mf} < u_s \quad (1)$$

Operation in the bubbling fluidized bed regime requires the superficial velocity to exceed the minimum velocity for bubbling:

$$u_{mb} < u_s \quad (2)$$

Finally, to prevent entrainment of particles, the slip velocity between gas and particles should not exceed the terminal or free-fall velocity of the particles:

$$u_{i,fl} - u_{i,p} < u_t \quad (3)$$

Criteria Eqs. (1)-(3) determine the range of gas velocities in which a fluidized bed of given particles can be operated. Correlations for the calculation of $u_{mf}$, $u_{mb}$ and $u_t$ as a function of the gas and particle properties are given in Annex I. Note that, in case particle entrainment cannot be totally avoided, cyclones can eventually be used and separated particles fed back into the bed.

In the bubbling fluidized bed regime, a bubble phase and an emulsion phase can be distinguished – this is the basis for the so-called two-phase model. For application of this model and evaluation of certain criteria, the calculation of the volume fraction of bubbles in the bed and of the bubble rise velocity is essential. Correlations are also given in Annex I.

### 2.2. Slugging and channelling

The reactor design must prevent the formation of large-scale non-uniformities such as slugging and channelling. In the case of slugging, bubbles are formed that grow and extend in the radial direction as they move upward, until they fill the full tube diameter [Werther, 1976a; Werther and Hartge, 2003]. With channelling, the fluidizing gas pierces through the bed at given locations, forming preferential paths, so-called channels, through which most of the gas flows towards the exit. Large-scale non-uniformities can be detected by deviations from the classical pressure drop-gas flow rate relation and/or fluctuations in the pressure drop. The occurrence of slugging or channelling results in

poor contact between gas and particles. In case of channelling, most of the gas completely bypasses the particle bed. With slugging, gas and particles are only mixed during the short time the slug reaches the freeboard surface. Such strongly non-ideal flow behaviour needs to be avoided.

Criterion to evaluate the risk for slugging:

Slugging can typically be avoided by reducing the height-to-diameter ratio of the bed. A rigorous criterion requires calculation of the evolution of the bubble diameter [Harrison and Leung, 1961]. For an orifice plate distributor, Darton [1977] derived:

$$d_b = \frac{0.54}{g^{\frac{1}{5}}}\left(u_s - u_{mf}\right)^{\frac{2}{5}}\left(z + 4\sqrt{A_0}\right)^{4/5} \quad (4)$$

with the $z$ the axial distance from the distributor ($\mathrm{m_r}$) and $A_0$ the orifice area of the plate ($\mathrm{m}^2$). For a porous plate distributor, Werther [1978] found:

$$d_b = 0.00853\left[1 + 27.2\left(u_s - u_{mf}\right)\right]^{\frac{1}{3}}(1 + 6.84z)^{1.21} \quad (5)$$

Correlation Eq. (5) was derived for Geldart B type solids and reported to be applicable for $d_t > 0.2\ m$, $0.01 \leq u_{mf} \leq 0.08\ m/s$, $100 \leq d_p \leq 350\ \mu m$, and $0.05 \leq u_s - u_{mf} \leq 0.3\ m/s$. Both expressions are valid up to $z_m$ where the bubble size is maximum – either the bed height or the height where the bubble size equals the reactor diameter. It is then considered that slugging can be avoided if the internal tube diameter, $d_t$, is larger than the bubble diameter at the end of the bed:

$$d_b(Z) < d_t \quad (6)$$

The criterion can be reformulated in terms of a required column height-to-diameter ratio:

for an orifice plate distributor: $\frac{0.54}{g^{\frac{1}{5}}}\left(u_s - u_{mf}\right)^{\frac{2}{5}} < \frac{d_t}{\left(Z+4\sqrt{A_0}\right)^{\frac{4}{5}}}$ (7)

for a porous plate distributor: $0.00853\left[1 + 27.2\left(u_s - u_{mf}\right)\right]^{\frac{1}{3}} < \frac{d_t}{(1+6.84Z)^{1.21}}$ (8)

Another criterion follows from measurements of the slug rise velocity by Stewart and Davidson [1965, 1967]. It was concluded that below a minimum bubble rise velocity, $u_{b,ms}$, slugging should not take place. A correlation was derived from the data as:

$$u_{b,ms} = u_{mf} + 7 \cdot 10^{-4}(g d_t)^{1/2} \qquad (9)$$

Elaborating on the observations of Stewart and Davidson [1965, 1967], Baeyens and Geldart [1974], carried out experiments with different columns and particles ($d_t$ = 5-30 cm, $\langle d_p \rangle$ = 55-3380 µm, $\rho_s$ = 850-2800 kg/m³) and concluded that complete slugging sets in at a given height:

$$z_s = 60 d_t^{0.175} \qquad (10)$$

with $z_s$ and $d_t$ in [cm]. Slugging can, hence, be expected if the bubble rise velocity, $u_{br}$, is higher than $u_{b,ms}$ and the bed has a height above $z_s$:

$$Slugging: \quad u_{br} > u_{b,ms} \quad AND \quad Z > z_s \qquad (11)$$

Correlations for the calculation of the bubble rise velocity, $u_{br}$, are given in Annex I.

Baeyens and Geldart [1974] also observed that it was more difficult to observe slugging in beds less than 0.3 m in height. An empirically modified correlation for Eq. (9) was proposed:

$$u_{b,ms} = u_{mf} + 7 \cdot 10^{-2}(g d_t)^{\frac{1}{2}} + 1.6 \cdot 10^{-3}\left(60 d_t^{0.175} - Z_{mf}\right)^2 \qquad (12)$$

where c.g.s. units (i.e. cm/g/s) instead of SI units (m/kg/s) are to be used. Yang [2003] showed a criterion for slugging based on a bubble coalescence model. Considering slugging occurs when the bubbles grow to the size of the vessel diameter:

$$\frac{Z}{d_t} > 3.5\left(1 - \frac{1}{\sqrt{N_o}}\right) \qquad (13)$$

<u>Criterion to evaluate the risk for channelling:</u>

Experiments with small particles [e.g. Behie et al., 1970, 1975, 1976] on jet penetration from gas distribution nozzles in fluidized beds indicate that only over a very short length, about half the nozzle diameter, the jet properties are similar to that at the jet nozzle. Channelling is, hence, closely related to a non-even distribution of the fluidizing gas over the bed and can in general be avoided by a well-

designed distributor providing sufficient pressure drop, $\Delta p_d$, compared to the pressure drop over the bed itself, $\Delta p_b$. A criterion for the minimum $\Delta p_d$ ensuring uniform fluidization was derived by Hiby [1964] based on experimental observations:

$$\Delta p_d/\Delta p_b = 0.15 \quad for \quad u_s/u_{mf} = 1-2 \qquad (14)$$

$$\Delta p_d/\Delta p_b = 0.015 \quad for \quad u_s/u_{mf} \gg 2$$

The criterion for a bed operated close to $u_{mf}$ was later confirmed by Siegel [1976] but stricter criteria were proposed by others. As a rule of thumb [Zuiderweg, 1967], an even distribution of the fluidizing gas is ensured when:

$$\Delta p_d \geq (0.2-0.4)\Delta p_b \qquad (15)$$

Karri and Knowlton [1999] recommend this criterion to be used with relatively tall beds (Z > 0.3 m) only. For shorter fluidized beds (Z < 0.3 m), the condition becomes more severe:

$$\Delta p_d \geq \Delta p_b \qquad (16)$$

Cocco et al. [2014] state that the pressure drop over a distributor or grid plate should ideally be at least 2500 Pa.

Studying bubbling fluidization of Geldart A particles with porous or perforated plate distributors ($u_s > u_{mb}$), Mori and Moriyama [1978] found that full fluidization requires:

$$\frac{\Delta p_d}{\Delta p_b} \geq \left(\frac{L_f}{L_{mf}} - 1\right)\frac{1}{1-(u_{mf}/u_s)^n} \qquad (17)$$

where $n = 1$ for porous plates and $n = 2$ for perforated plates. For porous plates at $u_s/u_{mf} > 10$ and for perforated plates at $u_s/u_{mf} > 3$, this equation reduces to:

$$\frac{\Delta p_d}{\Delta p_b} \geq \left(\frac{L_f}{L_{mf}} - 1\right) \qquad (18)$$

which further reduces to the rule of thumb found by Zuiderweg [1967], $\Delta p_d = (0.2-0.4)\Delta p_b$, if $L_f/L_{mf} = 1.2-1.4$, typical for a bubbling fluidized bed.

Extending the channelling model of Hiby [1964], Shi and Fan [1984] concluded that full fluidization can be guaranteed if:

$$(\Delta p_d + \Delta p_b)_{at\ any\ u_s} \cong (\Delta p_d + \Delta p_b)_{at\ u_{mf}} \qquad (19)$$

where:

$$\left(\frac{\Delta p_d}{\Delta p_b}\right)_{at\ u_{mf}} > \begin{cases} 0.14 & for\ porous\ plates \\ 0.07 & for\ perforated\ plates \end{cases} \quad (20)$$

Another, but similar, rule of thumb for achieving full and even fluidization and avoiding channelling is based on the velocity through the orifices or perforations of the distributor compared to the superficial velocity of the fluidizing gas. According to Kunii and Levenspiel [1991], the fraction of open or orifice area of a distributor plate, $A_o$, should be sufficiently small:

$$A_o < 0.1 \quad (21)$$

Note that the pressure drop over a distributor can e.g. be calculated according to the Darcy-Weisbach equation, which for laminar flow ($f_D$ = 64/*Re*) reduces to:

$$\Delta p_d = L_o \frac{128}{\pi} \frac{\mu F'}{N_o d_o^4} \quad (22)$$

The pressure drop over the bed, $\Delta p_b$, can be calculated according to Eq. (50), discussed later.

### 2.3. Axial dispersion

Kinetic modelling benefits greatly from an ideal-flow pattern, plug flow or well-mixed (referred to as CSTR – continuous stirred tank reactor). For the species in the bubble phase, plug flow needs to be approached, whereas for the species in the emulsion phase, either plug flow or complete mixing should be aimed at.

#### 2.3.1. Bubble phase: criterion for plug flow

Ideally, the motion of the bubbles through the bed can be described by a plug flow type model. This implies negligible axial dispersion in the bubble phase. $Pe'_{a,b}$, the bubble phase Peclet number based on column length $Z$ ($\mathrm{m_r}$), is defined as:

$$Pe'_{a,b} = \frac{f_b u_{br} Z}{D'_{ea,b}} \quad (23)$$

or:

$$Pe'_{a,b} = \frac{u_{br} Z}{D_{ea,b}} \quad (24)$$

with $D'_{ea,b}$ the bubble phase effective diffusivity in the axial direction ($\mathrm{m_f^3/m_r\ s}$). The effect of axial dispersion in the bubble phase can be assumed negligible if:

$$Pe'_{a,b} \gg 1 \tag{25}$$

Data and correlations for $Pe'_{a,b}$ for a wide range of column diameters were reported by Field and Davidson [1980] ($0.076\ m \leq d_t \leq 3.2\ m$) and Joshi [1980; 1982] ($0.092\ m \leq d_t \leq 1.067\ m$). A strong influence on the column diameter was observed. In commercial-size columns, back-mixing of bubbles is possible and can be significant. In small-diameter (lab-scale) reactors, the bubble phase is almost invariably in plug flow, with the gas in the emulsion phase in a regime between plug flow and well mixed [Froment et al., 2010]. According to Field and Davidson [1980]:

$$Pe'_{a,b} = \frac{f_b^{3.56} Z}{56.4 d_t^{1.33} (f_b u_{br})^{2.56}} = \frac{(u_s - u_{mf}) Z}{56.4 d_t^{1.33} u_{br}^{3.56}} = \frac{f_b^{3.56} Z}{56.4 d_t^{1.33} (u_s - u_{mf})^{2.56}} \tag{26}$$

Joshi [1982] reports:

$$Pe'_{a,b} = \frac{f_b u_{br} Z}{110 d_t^2 f_b u_{br}^2} = \frac{Z}{110 d_t^2 u_{br}} \tag{27}$$

The correlation of Field and Davidson [1980] typically gives somewhat lower values for $Pe'_{a,b}$ than the correlation of Joshi [1982].

The analysis based on the above defined Peclet numbers neglects partial back-mixing of gas bubbles that occurs when they reach the top of the bed. The effects of the latter on the observed reaction kinetics is considered small, as the reactions mostly take place in the dense emulsion phase. The effect of axial dispersion of the emulsion gas on the observed kinetics is also typically evaluated at the reactor inlet conditions, i.e. at the highest reaction rate in the reactor, as discussed hereafter.

### 2.3.2. Emulsion phase gas: criterion for plug flow or complete mixing

Due to the fluidization of the particle bed, the gas in the emulsion phase undergoes a certain degree of back-mixing. Two ideal situations that facilitate kinetic modelling are possible: the effect of back-mixing on the measured exit conversion is negligible, allowing using a plug flow model for the

emulsion gas; or back-mixing is dominant over convection, allowing use of a CSTR type model for the emulsion gas.

In the two-phase model, back-mixing in the emulsion phase is accounted for via an axial dispersion term in the emulsion phase species continuity equations:

$$f_e u_e \frac{\mathrm{d}C_{Ae}}{\mathrm{d}z} - f_e D_e \frac{\mathrm{d}^2 C_{Ae}}{\mathrm{d}z^2} - k_I(C_{Ab} - C_{Ae}) + r_A \rho_e (1 - f_b) = 0 \quad (28)$$

with boundary conditions:

$$-D_e \frac{\mathrm{d}C_{Ae}}{\mathrm{d}z} = u_e(C_{A0} - C_{Ae}) \text{ at } z = 0 \quad (29)$$

$$\frac{\mathrm{d}C_{Ae}}{\mathrm{d}z} = 0 \text{ at } z = Z$$

and where in case of bed dilution, $\rho_e$ can be calculated as $\rho_e = \rho_{s,cat}(1 - b_w)(1 - \varepsilon_e)$.

Two criteria have been derived to evaluate if these general second-order differential equations can be simplified in order to be able to carry out the parameter estimation for the intrinsic reaction kinetics with a negligible effect of the exact value of $D_e$ and to reduce the computation time. The first criterion assesses if axial dispersion is sufficiently small to justify use of a plug flow model. The second criterion verifies if axial dispersion is dominant, allowing the use of the CSTR model. The criterion for negligible axial dispersion compares the conversion obtained when accounting and not accounting for axial dispersion [Young and Finlayson, 1973]. Reactor inlet conditions are considered for the comparison, assuming that they imply maximum reaction rates in the reactor and as such a maximum potential effect of axial dispersion. The criterion for dominant axial dispersion compares the conversion immediately downstream of the reactor inlet (z = 0) and at the reactor outlet.

Considering the extreme case, where bubble-emulsion phase species transport does not limit consumption or production of species by reaction, the emulsion phase species continuity equations for a (pseudo-) first order reaction can be written in dimensionless variables as:

$$\gamma \frac{\mathrm{d}^2 x_{Ae}}{\mathrm{d}z'^2} - \frac{\mathrm{d}x_{Ae}}{\mathrm{d}z'} + \beta r_{A0}(1 - x_{Ae}) = 0 \quad (30)$$

with boundary conditions:

$$\gamma \frac{\mathrm{d}x_{Ae}}{\mathrm{d}z'} = x_{Ae} \text{ at } z' = 0 \quad (31)$$

$$\gamma \frac{\mathrm{d}x_{Ae}}{\mathrm{d}z'} = 0 \text{ at } z' = 1$$

The dimensionless variables are defined as:

$$z' = \frac{z}{Z} \tag{32}$$

$$x_{Ae} = \frac{C_{A0} - C_{Ae}}{C_{A0}}$$

$$\gamma = \frac{D_e}{u_e Z}$$

$$\beta = \frac{\rho_e (1 - f_b) Z}{u_e f_e C_{A0}}$$

and $r_{A0}$ is the reaction rate at the reactor inlet (z = 0). Apart from the correlation to be used for the effective diffusivity, $D_e$, the equation is similar to that for a fixed bed reactor for which an analytical solution was derived by Wehner and Wilhelm [1956]:

$$x(z) = 1 - \frac{2e^{\frac{z}{2\gamma}}\left((1+a)\mathrm{e}^{\frac{a(1-z)}{2\gamma}} - (1-a)\mathrm{e}^{\frac{a(z-1)}{2\gamma}}\right)}{(1+a)^2 e^{\frac{a}{2\gamma}} - (1-a)^2 e^{\frac{-a}{2\gamma}}} \text{ with } a = \sqrt{1 + 4\beta\gamma r_{A0}} \tag{33}$$

Correlations for the effective diffusivity in the emulsion phase, $D_e$, are given in Annex I.

<u>Criterion justifying plug flow description for the emulsion phase gas:</u>

When the effect of axial dispersion is negligible, at the reactor inlet, $z \rightarrow 0$, Eq. (33) reduces to:

$$x_{Ae1}(0) = 1 - \frac{1}{1 + \gamma\beta r_{A0}} \tag{34}$$

The true plug flow solution follows from solving a plug flow species continuity equation for the emulsion phase:

$$-\frac{\mathrm{d}(f_e u_e C_{Ae})}{dz} = r_A \rho_e (1 - f_b) \overset{\Delta}{\rightarrow} \frac{\mathrm{d}x_{Ae}}{dz'} - \beta r_{A0}(1 - x_{Ae}) = 0 \tag{35}$$

with boundary condition:

$$C_{Ae} = C_{A0} \text{ at } z = 0 \overset{\Delta}{\rightarrow} x_{Ae} = 0 \text{ at } z' = 0 \tag{36}$$

The solution of this equation, $\mathrm{x_{Ae2}} = 1 - \mathrm{e}^{-\beta \mathrm{r_{A0}} \mathrm{z}'}$, gives at the reactor inlet:

$$\mathrm{x_{Ae2}}(0) = 0 \tag{37}$$

Comparing $x_{Ae1}(0)$ and $\mathrm{x_{Ae2}}(0)$, a criterion for negligible axial dispersion then becomes:

$$x_{Ae1}(0) - x_{Ae2}(0) = \frac{\gamma\beta r_{A0}}{1+\gamma\beta r_{A0}} \cong \gamma\beta r_{A0} \ll 1 \qquad (38)$$

The criterion can be rewritten in terms of the particle diameter-based Peclet number of the emulsion gas, $Pe_{a,eg}$:

$$Pe_{a,eg} = \frac{\mathrm{d}_p u_e}{D_e} \gg \frac{\rho_e(1-f_b) r_{A0} d_p}{u_e f_e C_{A0}} \qquad (39)$$

Accounting for the integrated effect of axial dispersion over the reactor, Mears [1971] and Gierman [1988] proposed:

$$Pe_{a,eg} > \frac{8 d_p}{\mathrm{Z}} n ln\left(\frac{1}{1-x_A}\right) \qquad (40)$$

<u>Criterion justifying considering complete mixing for the emulsion phase gas:</u>

If a CSTR behaviour is justified, the conversion makes a jump as the flow enters the reactor and the difference between the conversion in the immediate vicinity of the reactor inlet and at the reactor outlet is small. From the general solution of the dimensionless emulsion phase species continuity equations, Eq. (33):

$$x_{Ae}(0) = 1 - \frac{2\left[(1+a)\mathrm{e}^{\frac{a}{2\gamma}} - (1-a)\mathrm{e}^{\frac{-a}{2\gamma}}\right]}{(1+a)^2\mathrm{e}^{\frac{a}{2\gamma}} - (1-a)^2\mathrm{e}^{\frac{-a}{2\gamma}}} = \frac{\left(1-a^2\right)\left(1-\mathrm{e}^{\frac{a}{\gamma}}\right)}{(1+a)^2\mathrm{e}^{\frac{a}{\gamma}} - (1-a)^2} \qquad (41)$$

and:

$$x_{Ae}(1) = 1 - \frac{4a\mathrm{e}^{\frac{1+a}{2\gamma}}}{(1+a)^2\mathrm{e}^{\frac{a}{\gamma}} - (1-a)^2} = \frac{(1+a)^2\mathrm{e}^{\frac{a}{\gamma}} - (1-a)^2 - 4a\mathrm{e}^{\frac{1+a}{2\gamma}}}{(1+a)^2\mathrm{e}^{\frac{a}{\gamma}} - (1-a)^2} \qquad (42)$$

Introducing a maximum acceptable relative error between the observed and intrinsic reaction rates, $\Delta r_{rel}$, a criterion to verify CSTR behaviour can be written:

$$\left|\frac{x_{Ae1}(1) - x_{Ae1}(0)}{x_{Ae1}(1)}\right| = \left|\frac{2\left((1+a)\mathrm{e}^{\frac{a}{\gamma}} - (1-a) - 2a\mathrm{e}^{\frac{1}{2\gamma}}\right)}{(1+a)^2\mathrm{e}^{\frac{a}{\gamma}} - (1-a)^2 - 4a\mathrm{e}^{\frac{(1+a)}{2\gamma}}}\right| < \Delta r_{rel} \qquad (43)$$

A typical value for $\Delta r_{rel}$ is 0.05.

### 2.3.3. Emulsion phase particles: criterion for complete mixing

Particles can react or participate in the reaction, e.g. as catalyst. The fluidized state ensures a certain degree of mixing of the particles, but whether complete mixing can be assumed depends on how the mixing and reaction time scales compare. In case of continuous solids feeding and removal or in case the particles react, the average residence time of the particles often scales with the reaction time scale. On that basis, Baeyens and Geldart [1973] and Geldart [1986] derived a criterion comparing the bed turnover or mixing time and the average residence time of the particles in the bed. A true comparison between mixing and reaction time scales is not made, so that the criterion is a necessary but not sufficient condition for assuming complete mixing. Geldart [1986] derived a correlation for the solids' circulation flux, $J$, in a fluidized bed:

$$J = \rho_s(1-\varepsilon_{mf})(u_s - u_{mf})Y(\beta_w + 0.38\beta_d) \qquad (44)$$

The factor 0.38 is based on experimental observations showing that the particles that are carried up by the drift flux move on average at about 38% of the bubble velocity. The parameters Y, $\beta_w$ and $\beta_d$ account for respectively deviation from two-phase theory, the wake and the drift fraction and are material dependent. Values for some common materials can be extracted from Figure 2. A semi-empirical correlation not requiring values of such parameters was derived by Werther [1976b] based on measurements of the bubble properties in a 1 m-diameter bed:

$$J = 0.67\rho_s(1-\varepsilon_{mf})(u_s - u_{mf})\left(\frac{1}{\phi_b} - 1\right) \qquad (45)$$

with the bubble shape factor, $\phi_b$:

$$\phi_b = \{1 - 0.3\mathrm{EXP}[-8(u_s - u_{mf})]\}e^{-\omega z} \qquad (46)$$

and:

$$\omega = 7.2(u_s - u_{mf})\mathrm{EXP}[-4.1(u_s - u_{mf})] \qquad (47)$$

Correlation Eqs. (45)-(47) was found satisfactory for $1115 \leq \rho_s \leq 2624\ \mathrm{kg_p/m_p^3}$, $100 \leq d_p \leq 635\ \mu\mathrm{m}$, $0.02 \leq u_{mf} \leq 0.24\ \mathrm{m_f^3/m_r^2/s}$ and $(u_s - u_{mf}) \leq 0.80\ \mathrm{m_f^3/m_r^2/s}$. The bed turnover time, $t_T$, can then be calculated from [Geldart, 1986]:

$$t_T = Z_{mf}\rho_s\left(1-\varepsilon_{mf}\right)/J \tag{48}$$

in which Eq. (44) or Eqs. (45)-(47) can be substituted.

### 2.4. Criterion for isobaric operation

To facilitate kinetic modelling, pressure differences over the bed should be kept sufficiently small. A common criterion for the maximum allowable pressure drop is:

$$\Delta p_b < 0.2\frac{p_t}{n} \tag{49}$$

with $p_t$ the operating pressure and $n$ the reaction order. The pressure drop over the bed, $\Delta p_b$, is determined by the pressure drop required for minimum fluidization of the bed, dominated by the hydrostatic contribution. Furthermore, beyond the minimum fluidization flow rate, the pressure drop over the bed does not vary much until entrainment starts [Kunii and Levenspiel, 1991], so that $\Delta p_b$ can be calculated as:

$$\Delta p_b = L_{mf}\left(1-\varepsilon_{mf}\right)\left(\rho_s-\rho_g\right)g \tag{50}$$

## 3. ISOTHERMAL OPERATION

### 3.1. Radial temperature gradient

Isothermal operation requires negligible radial temperature differences or heat transport limitations in the bed. This typically requires dilution of the bed with inert particles, but segregation of catalyst / reacting particles and diluent particles is to be avoided, e.g. by using deactivated catalyst. Criteria for fluidized beds can be derived in a similar way than those for fixed beds [Mears, 1971a; 1971b]. The criteria are based on a maximum allowable relative difference between the reaction rate in the immediate vicinity of the wall and the radially averaged reaction rate in the bed. This difference must be smaller than the maximum allowable relative error on the observed reaction rate, $\Delta r_{rel}$:

$$\frac{\overline{r_A}-r_{A,w}}{r_{A,w}} < \Delta r_{rel} \tag{51}$$

, with a typical value for $\Delta r_{rel}$ of 0.05.

The criteria are derived starting from the steady state heat balance, considering the extreme case without axial convection and focusing on the axial position where the cold or hot spot is most likely located. The detailed derivations are given in Annex II.

Based on Eq. (51), a first criterion can be derived in case the heat transfer resistance at the wall, i.e. over the near-wall boundary layer, can be neglected, typically justified for $d_t/d_p > 100$:

$$\Delta T_{c,w} = \frac{|-\Delta H| r_A(T_w) \rho_B d_t^2}{16 \lambda_{er}} < \Delta r_{rel} \frac{2RT_w^2}{E} \tag{52}$$

where $\Delta T_{c,w}$ represents the temperature difference between the centre of the bed and the inner wall (K). The second criterion accounts for dominant heat transfer limitations in the near wall region and is typically applied $d_t/d_p < 100$:

$$\Delta T_{c,w} = \left(1 + \frac{8}{Bi_w} \frac{r_p}{R_t}\right) \frac{|-\Delta H| r_A(T_w) \rho_B d_t^2}{16 \lambda_{er}} < \Delta r_{rel} \frac{2RT_w^2}{E} \tag{53}$$

or:

$$\Delta T_{c,w} = \left(1 + \frac{8}{\widetilde{Bi_w}}\right) \frac{|-\Delta H| r_A(T_w) \rho_B d_t^2}{16 \lambda_{er}} < \Delta r_{rel} \frac{2RT_w^2}{E} \tag{54}$$

Criterion Eqs. (53) or (54) can only be strictly applied if the temperature of the tube wall is measured. The two criteria for negligible radial temperature gradients require correlations for the effective thermal conductivity in the radial direction, $\lambda_{er}$, and the convective heat transfer coefficient in the vicinity of the wall, $\alpha_w$. Correlations for bubbling fluidized beds are provided in Annex I.

### 3.2. Bed dilution – fluidization and segregation

In case bed dilution with inert particles is needed to achieve isothermal operation, catalyst and inert particles have to be well mixed and excessive dilution must be avoided to ensure that all fluid elements encounter about the same amount of catalyst on their way from the inlet to the exit of the reactor and no bypassing can occur. For fixed bed reactors, an expression for the maximum allowable bed dilution $\left[m_{inert}^3/m_s^3\right]$ was derived by Berger et al. [2002]:

$$b < \frac{\Delta x_{rel}}{\Delta x_{rel} + \frac{0.5 n x_A d_p}{L}} \tag{55}$$

where $\Delta x_{rel}$ represents the maximum acceptable relative deviation of the conversion (%), typically 0.05, $n$, the reaction order, and $x_A$, the conversion of A. The latter can be analytically or numerically calculated, depending on the nature of the reaction kinetics.

For fluidized bed reactors, criterion Eq. (55) may be too severe. Catalyst and inert particles are continuously mixed, increasing the probability of all fluid elements encountering the same amount of catalyst on their way through the reactor. Nevertheless, segregation of catalyst and inert particles needs to be avoided. A first evaluation of potential segregation problems follows from comparing the minimum fluidization velocity of the catalyst and inert particles – see correlations presented in Annex I. A second approach is based on the comparison of the beginning fluidization velocity, $u_{bf}$, and the total fluidization velocity, $u_{tf}$. At the beginning fluidization velocity, finer / lighter particles start to fluidize, whereas at the total fluidization velocity all particles, including the larger / heavier ones, are fluidized. Phase equilibrium type diagrams can be constructed [Kondukov and Sosna, 1965; Gelperin et al., 1967], such as shown in Figure 3 [Yang, 2003; Adapted from Chen and Keairns, 1975]. Equations for the beginning and total fluidization velocity were proposed by Vaid and Sen Gupta [1978]:

$$Re_{bf} = \frac{d_p u_{bf} \rho_f}{\mu} = [(18.1)^2 + 0.0192Ar]^{0.5} - 18.1 \qquad (56)$$

$$Re_{tf} = \frac{d_p u_{tf} \rho_f}{\mu} = [(24.0)^2 + 0.0546Ar]^{0.5} - 24.0 \qquad (57)$$

with $Ar$ the Archimedes number defined as:

$$Ar = \frac{\rho_f d_p^3 (\rho_s - \rho_f) g}{\mu^2} \qquad (58)$$

It is important to notice that reaching total fluidization is no guarantee for particle mixing or negligible segregation. At $u_{tf}$, the bed may be totally fluidized, but far from perfectly mixed [Yang, 2003].

A criterion for negligible segregation is challenging to derive, especially as catalyst and inert typically show a particle size distribution. A general qualitative classification to know which of the particles will have a tendency to sink (jetsam) and which to float (flotsam) was presented by Chiba et

al. [1980], as shown in Figure 4. In a multi-component system, a particular particle may be a flotsam with respect to given particles and jetsam with respect to others. It was also observed that in general, the distinction flotsam-jetsam is less important in multi-component systems with density differences [Yang, 2003]. The literature has no clear recommendation to work with catalyst and inert particles of equal size or weight. Ideally, inert particles with the same particle size distribution and other physical properties than the catalyst are produced by deactivating the catalyst somehow. Mathematical models have been proposed to calculate the equilibrium concentration profiles in multi-component gas fluidized beds. Simple quantitative segregation equations can only be formulated for binary systems with nearly spherical particles [Yang, 2003]. Rowe et al. [1972] derived the following equation to evaluate the tendency for segregation in terms of the properties of the flotsam (F) and jetsam (J) particles and the big (B) and small (S) particles:

$$Segregation\ tendency\ \propto \left[u_s - \left(u_{mf}\right)_F\right]\left[\frac{(\rho_s)_J}{(\rho_s)_F}\right]^{-2.5}\left[\frac{(d_p)_B}{(d_p)_S}\right]^{-0.2} \qquad (59)$$

It is worth noticing that segregation by particle density differences is more pronounced than by particle size differences and that the exact influence of the gas velocity is still to be determined. Particle size differences mainly alter the minimum fluidization velocity of the mixture – see Annex I. A normalized segregation tendency that should be close to 1 can then be defined as:

$$Normalized\ segregation\ tendency\ \propto \left[\frac{(\rho_s)_J}{(\rho_s)_F}\right]^{-2.5}\left[\frac{(d_p)_B}{(d_p)_S}\right]^{-0.2} \qquad (60)$$

Pielsticker et al. [2018] recommend using particles of similar Archimedes number to promote fast and homogeneous mixing of catalyst or reacting particles and inert diluent particles over the entire bed height and to prevent entrainment of the less dense or lighter particles with the gas.

### 3.3. Adiabatic temperature rise

In addition to assessing radial temperature gradients, it is interesting to calculate the adiabatic temperature rise over the reactor. The latter gives an indication of how challenging isothermal operation will be and follows from:

$$\Delta T_{ad} = \frac{|-\Delta H| y_{A0} x_A}{c_{P,f} M_m} \quad (61)$$

## 4. INTERFACIAL TRANSFER

Measuring intrinsic reaction kinetics requires negligible interfacial mass and heat transfer limitations. For gas-solids mass and heat transfer, criteria developed by Mears [1971a; 1971b] can be adopted with the appropriate correlations for the mass and heat transfer coefficients. Mass transfer between the bubble and emulsion phase is, however, typically critical in bubbling fluidized bed reactors. A criterion for bubble-emulsion mass transfer limitations similar to the criteria of Mears [1971a; 1971b] is presented hereafter.

### 4.1. Bubble-emulsion mass transfer

Sufficiently small species concentration differences between the bubble and emulsion phases can justify the use of a pseudo-homogeneous reactor model. To develop a criterion, two cases are distinguished. For the bubble phase, plug flow of the gas is assumed. For the emulsion phase, either plug flow of the gas or complete back mixing are considered. Which of these two applies is to be verified as discussed in the section on Axial dispersion.

Consider a reaction rate:

$$r_A = \mathrm{k}\, f(C_A) \qquad \text{with:} \qquad f(C_A) = C_A^n \quad (62)$$

Assuming bubble-emulsion phase mass transfer and reaction are the dominant phenomena and considering a local equilibrium between the rates of interphase mass transfer and reaction:

$$r_A(C_{Ab})\rho_b f_b + k_I(C_{Ab} - C_{Ae}) = r_A(C_{Ae})\rho_e(1 - f_b) - k_I(C_{Ab} - C_{Ae}) \quad (63)$$

The concentration difference between the bubble and emulsion phases can then be written:

$$(C_{Ab} - C_{Ae}) = \frac{[r_A(C_{Ae})\rho_e(1-f_b) - r_A(C_{Ab})\rho_b f_b]}{2k_I} \quad (64)$$

<u>Emulsion phase gas in plug flow:</u>

For the case where the gas in the emulsion phase is in plug flow, like the bubble phase, a relative error on the species concentration can be developed in terms of a first order Taylor series around $C_{Ab}$:

$$r_A(C_{Ae}) = r_A(C_{Ab})\left(1 + n\frac{C_{Ae}-C_{Ab}}{C_{Ab}}\right) \tag{65}$$

so that:

$$\frac{r_A(C_{Ab})-r_A(C_{Ae})}{r_A(C_{Ab})} = n\frac{C_{Ab}-C_{Ae}}{C_{Ab}} < RI_{im,r} \tag{66}$$

with $n$ the reaction order and $RI_{im,r}$ the maximum allowable relative influence of bubble-emulsion phase mass transfer on the observed reaction rate (%). Introducing Eq. (64) in Eq. (66):

$$\frac{r_A(C_{Ab})-r_A(C_{Ae})}{r_A(C_{Ab})} = n\frac{C_{Ab}-C_{Ae}}{C_{Ab}} = \frac{n[r_A(C_{Ae})\rho_e(1-f_b)-r_A(C_{Ab})\rho_b f_b]}{2k_I C_{Ab}} < RI_{im,r} \tag{67}$$

In the case of plug flow, the condition is to be tested under the most severe conditions, that is, at the highest possible reaction rate. Therefore, reactor inlet conditions are substituted in Eq. (67):

$$\frac{r_A(C_{Ab})-r_A(C_{Ae})}{r_A(C_{Ab})} \cong \frac{n[r_A(C_{A0})\rho_e(1-f_b)-r_A(C_{A0})\rho_b f_b]}{2k_I C_{A0}} < RI_{im,r} \tag{68}$$

With negligible catalyst and reaction in the bubble phase, Eq. (68) simplifies to:

$$\frac{nr_A(C_{A0})\rho_e(1-f_b)}{2k_I C_{A0}} < RI_{im,r} \tag{69}$$

Emulsion phase gas well-mixed:

In case the gas in the emulsion phase is well-back mixed, with the bubble phase assumed to be in plug flow and developing the first order Taylor series around $C_{Ae}$, the criterion becomes:

$$\left|\frac{r_A(C_{Ae})-r_A(C_{Ab})}{r_A(C_{Ae})}\right| = \left|n\frac{C_{Ae}-C_{Ab}}{C_{Ae}}\right| < RI_{im,r} \tag{70}$$

Introducing Eq. (64) into Eq. (70) gives:

$$\left|\frac{r_A(C_{Ae})-r_A(C_{Ab})}{r_A(C_{Ae})}\right| = \left|n\frac{[r_A(C_{Ab})\rho_b f_b - r_A(C_{Ae})\rho_e(1-f_b)]}{2k_I C_{Ae}}\right| < RI_{im,r} \tag{71}$$

Accounting for negligible reaction in the bubble phase, this reduces to:

$$\left|\frac{r_A(C_{Ae})-r_A(C_{Ab})}{r_A(C_{Ae})}\right| = \left|\frac{-nr_A(C_{Ae})\rho_e(1-f_b)}{2k_I C_{Ae}}\right| < RI_{im,r} \tag{72}$$

$C_{Ae}$ in the denominator of Eq. (72) can be expressed in term of $C_{A0}$ and the reaction rate $r_A(C_{Ae})$ by solving the species continuity equation:

$$F_A^{IN} - F_A^{OUT} = r_A \rho_e (1 - f_b) V \tag{73}$$

or:

$$(f_b u_b + f_e u_e)(C_{A0} - C_{Ae}) \Omega = r_A(C_{Ae}) \rho_e (1 - f_b) \Omega Z \tag{74}$$

Hence:

$$C_{Ae} = C_{A0} - r_A(C_{Ae}) \frac{\rho_e (1 - f_b) Z}{f_b u_b + f_e u_e} \tag{75}$$

Note that Eq. (75) is an implicit equation in $C_{Ae}$. Substituting Eq. (75) in Eq. (72) results in:

$$\left| \frac{r_A(C_{Ae}) - r_A(C_{Ab})}{r_A(C_{Ae})} \right| = \left| \frac{-n r_A(C_{Ae}) \rho_e (1 - f_b)}{2 k_I \left[ C_{A0} - r_A(C_{Ae}) \frac{\rho_e (1 - f_b) Z}{f_b u_b + f_e u_e} \right]} \right| < RI_{im,r} \tag{76}$$

In the absence of bubble-emulsion phase mass transfer limitations in the reactor, the emulsion phase concentration, $C_{Ae}$, can be replaced by the average concentration in the reactor, $\overline{C_A}$, so that the criterion for negligible bubble-emulsion phase mass transfer limitations with a well-mixed emulsion phase finally becomes:

$$\left| \frac{-n r_A(\overline{C_A}) \rho_e (1 - f_b)}{2 k_I \left[ C_{A0} - r_A(\overline{C_A}) \frac{\rho_e (1 - f_b) Z}{f_b u_b + f_e u_e} \right]} \right| < RI_{im,r} \tag{77}$$

Criteria Eq. (68)/(69) and Eq. (77) require a correlation for the interchange coefficient for mass transfer between the bubble and emulsion phase, $k_I$. Frequently used correlations are given in Annex I.

### 4.2. Gas-solid heat and mass transfer

Reaction rates depend strongly on the temperature and it is important to guarantee that the bulk temperature that is measured is representative for the temperature at the locus of reaction, i.e. in the solid. Intra-particle thermal conduction is typically fast so that the major concern is to make sure that gas-solid heat transfer limitations are negligible. The criterion that can be used is similar to the one developed for fixed bed reactors by Mears [1971a; 1971b]:

$$\Delta T_{s,f} = \frac{(-\Delta H) r_A \rho_s d_p}{6 \mathrm{h}_f} < \Delta r_{rel} \frac{R T_B^2}{E} \qquad (78)$$

where $\Delta \mathrm{T}_{\mathrm{s,f}}$ is the temperature difference between the solid surface and the bulk fluid (K). The derivation is shown in Annex III. The reaction rate, $r_A$, can be calculated with the bulk concentration, $C_{AB}$, and bulk temperature, $T_B$, assuming absence of gas-solid mass and heat transfer limitations and bubble-emulsion phase transport limitations. Application of criterion Eq. (78) requires a correlation for the gas-solid heat transfer coefficient, $\mathrm{h}_f$. Annex I provides some widely used correlations.

Identifying the relation between the reaction conditions – at the locus of reaction – and the reaction rates also requires negligible gas-solid mass transfer limitations. The derivation, given in Annex III, is similar to the one presented by Mears [1971a; 1971b] for fixed bed reactors and yields:

$$\Delta \mathrm{C}_{\mathrm{A,es}} \approx \Delta \mathrm{C}_{\mathrm{A,fs}} = \frac{r_A \rho_s d_p}{6 k_g} < R I_{im,r} \frac{C_{A,e}}{n} \qquad (79)$$

where $\Delta \mathrm{C}_{\mathrm{A,es}}$ is the concentration difference between the emulsion fluid and the solid surface and $\Delta \mathrm{C}_{\mathrm{A,fs}}$ is the concentration difference between the bulk fluid and the solid surface. The reaction rate, $r_A$, can be calculated with the bulk concentration, $C_{AB}$, and bulk temperature, $T_B$, assuming absence of gas-solid mass and heat transfer limitations and bubble-emulsion phase transport limitations. Frequently used correlations for the calculation of the gas-solids mass transfer coefficient, $k_g$, are given in Annex I.

**5. INTRA-PARTICLE HEAT AND SPECIES TRANSPORT**

The criteria for negligible intra-particle heat and species transport limitations that have been derived for fixed bed reactors can be used as such. The derivation is shown in Annex IV. Nevertheless, as the particles used in fluidized bed reactors, and in particular fluidized bed reactors for studying reaction kinetics, are typically smaller in diameter than the particles used in a fixed bed reactor, intra-particle transport limitations are less likely.

A criterion for negligible intra-particle heat transport limitations is based on a maximum relative error on the measured reaction rate [Anderson, 1963; Mears, 1971a; 1971b]:

$$\sigma = \Delta T_{c,s} = \frac{(-\Delta H)\bar{r}_A \rho_s d_p^2}{24\lambda_e} < \Delta r_{rel} \frac{5RT_s^2}{2E} \quad (80)$$

where $\Delta T_{c,s}$ is the temperature difference between centre and the external surface of the particle.

Weisz and Prater [1954] developed a criterion to evaluate negligible intra-particle species transport limitations. The criterion was originally developed for a slab of catalyst but extended to other geometrical shapes. Negligible intra-particle species transport limitations are ensured provided that:

$$\frac{(n+1)\overline{r_A}\rho_s}{2a_g^2 D_{eA} C_{A,s}^s} < 0.33 \quad \text{for n} = 0 \quad (81)$$

$$\frac{(n+1)\overline{r_A}\rho_s}{2a_g^2 D_{eA} C_{A,s}^s} < 0.08 \quad \text{for n} \geq 0.5 \quad (82)$$

Note that with certain reactions, pellet-scale mass transfer limitations are irreducible [Couwenberg et al., 1996]. A Boudart number based criterion can in such case be used, as proposed by Vandewalle et al. [2021].

## 6. CASE STUDY

The case study that is presented aims at illustrating the main difficulties that one can expect to encounter when using a laboratory bubbling fluidized bed to determine the intrinsic reaction kinetics of a heterogeneous catalytic reaction. The highly endothermic Steam Methane Reforming (SMR) reaction is taken as an example. When using a micro-packed bed reactor to study SMR, isothermal operation is challenging, even when diluting the catalyst bed. As a result, measurements of the intrinsic reaction kinetics can be carried out at temperatures below ca. 550-600°C only, depending on the activity of the catalyst [Xu and Froment, 1989; Minette et al., 2018]. Extrapolation of the reaction kinetics to commercial operating temperatures of up to 900°C then requires determining the activation energies of the reactions with sufficient precision, using data in a sufficiently wide temperature range. This may require experiments with the reverse reaction – methanation – both costly and time consuming.

Using a micro-(bubbling) fluidized bed (MFB) reactor, with excellent heat transport properties, can facilitate isothermal operation and has therefore been proposed to study SMR. For the case study, the work of Chen et al. [2020] is considered in which a 20 mm ID MFB was used to study SMR kinetics on a Ni-catalyst. Bed dilution was applied, not only to improve isothermal operation, but to attempt preventing chemical equilibrium is reached within the reactor so that reaction kinetics can be derived from the data. A mixture of quartz sand and catalyst was fluidized at superficial velocities around 6 x $u_{mf}$. Experiments were carried out in a very wide temperature range, 500-800°C, and at 2 bara. Key data for the Case study are reproduced in Figure 6. Although not rigorously verified, it was assumed that interfacial mass and heat transfer limitations could be ignored, and operation was isothermal. Working with 75-96 µm catalyst particles, intra-particle diffusion limitations were also considered negligible. Activation energies smaller than those reported in the literature were measured, which the authors attributed to a higher NiO content of the catalyst used. Physicochemical testing of the parameters was not addressed.

To evaluate all the criteria that ensure that intrinsic reaction kinetics is measured, some realistic assumptions had to be made on the unreported bed dilution ratio and gas distributor design. For the evaluation, a reported total volumetric flow rate of $1.2 \cdot 10^{-5}$ $m^3_g/s$ was imposed, with a $H_2O/CH_4$ molar feed ratio of 3, a $H_2/CH_4$ molar feed ratio of 0.005 and 60 vol% dilution with $N_2$. The molar feed flow rate of $CH_4$ is then $2.96 \cdot 10^{-5}$ $mol_{CH4}/s$. Spherical particles with a mean diameter of 85 µm and density of 1550 $kg_{cat}/m^3_{cat}$ were considered. The authors report $2.94 \cdot 10^{-3}$ kg of catalyst was used and 85% bed dilution is assumed to come to an acceptable bed height.

The calculated superficial gas velocity is ca. $3.8 \cdot 10^{-2}$ $m^3_g/m^2_r/s$, which is 7.8 times the calculated minimum fluidization velocity of $4.9 \cdot 10^{-3}$ $m^3_g/m^2_r/s$ and well below the terminal velocity of $1.1 \cdot 10^{-1}$ $m_r/s$. With that, the bubble volume fraction in the bed is calculated to be 0.33 $m^3_b/m^3_r$, with an average bed void fraction of 0.60 $m^3_g/m^3_r$ and the bed expanding to $1.0 \cdot 10^{-1}$ $m_r$ with an acceptable pressure drop of 612 Pa. For the gas distributor, the size of the perforations must not exceed the particle diameter. The gas distributor was assumed to consist of 1500 perforations with an 85 µm

diameter. With that, the fraction open area is 2.7% of the bed cross sectional surface area, well below the recommended maximum 10%. Avoiding channeling essentially depends on the pressure drop over the gas distributor. The criterion shows that with the given bed characteristics and number of perforations and size, a $5 \cdot 10^{-3}$ m thick gas distributor needs to be used to ensure a pressure drop over the gas distributor higher than that over the bed and prevent channeling. A sintered wire mesh filter can e.g. be used. Absence of slugging is confirmed, with the maximum bubble diameter just below that of the tube and the theoretical height at which slugging sets in is with $6.8 \cdot 10^{-1}$ $m_r$ also well above the bed height. The evaluation of transport limitations depends on the intrinsic reaction rate and is, hence, uncertain when using the observed reaction rate as reported by Chen et al. [2020] for the calculations. Allowable concentration and temperature differences are based on the acceptable relative difference between the observed and intrinsic reaction rates, which was set at 5%. First considering the observations at 500°C, a reaction rate of the order $3*10^{-5}$ kmol/$kg_{cat}$/s is reported for the main SMR reaction with the imposed reaction conditions (S/C-ratio = 3.0). As for the effect of axial dispersion, the axial Péclet number for the bubble phase is with a value of 13-39, depending on the correlation that is used, well above 1, so that plug flow can be assumed for the bubble phase. For the emulsion phase gas, on the other hand, the axial Péclet number is too small to justify plug flow. Perfect mixing of the emulsion gas can be assumed and results in a 2.8% relative difference between the observed and intrinsic reaction rates, well below the acceptable 5%. With an estimated inner reactor wall temperature of 550°C, the radial temperature difference in the bed is less than 0.1 K and well below the allowable 2.35 K. The criteria for intra-particle species diffusion and heat transport limitations show intra-particle concentration and temperature differences well below the allowable values. The Weisz-Prater [1954] criterion gives a value Φ of $8.4 \cdot 10^{-4}$ as compared to the allowable 0.08. The intra-particle temperature difference is estimated to be 0.01 K compared to the allowable 2.6 K. As for gas-solid mass and heat transfer limitations, the Mears [1971] criteria seem satisfied with the gas-solid methane concentration difference estimated to be $2.7 \cdot 10^{-6}$ kmol/$m^3_g$, well below the allowable $1.6 \cdot 10^{-4}$ kmol/$m^3_g$, and the gas-solid temperature difference estimated to be 0.04-0.7 K

depending on the $j_H$-correlation used, smaller than the allowable 1.0 K. The criterion for bubble-emulsion mass transfer with well-mixed emulsion gas, indicates a significantly higher than acceptable relative difference between the observed and intrinsic reaction rates with a value of 20%. Because this value is calculated based on the observed reaction rate, the true difference will be even higher. Note that for the given operating conditions, a value of 1.8 $m^3_g/m^3_r/s$ was obtained using the correlation of Kunii and Levenspiel [1969, 1991] with the mean bubble diameter in the bed – a realistic value for the small particles that are used [Medrano et al., 2017a; 2017b]. Table 1 summarizes the results of the evaluation at 500°C using the observed reaction kinetics and allowing 5% relative error between observed and intrinsic reaction kinetics. From the above, it can be concluded that bubble-emulsion phase mass transfer limitations were probably encountered in the experiments. It could explain the relatively low reaction rates, more than two orders of magnitude lower than measured by Xu and Froment [1989] for a commercial Ni-based SMR catalyst. Furthermore, Chen et al. [2020] report the main SMR reaction rate to increase quasi-linearly by ca. a factor 4 when increasing the temperature from 500°C to 700°C, with only a small to no further increase when going to 750°C and 800°C. This could be due to bubble-emulsion phase mass transfer limitations becoming more limiting as the intrinsic reaction rate increases exponentially with temperature. With a reported methane conversion of 92.28% at 800°C, the reactor may have been operated in a totally bubble-emulsion phase mass transfer limited regime or the SMR reactions may have approached equilibrium. Extracting intrinsic reaction kinetics from the data is then not possible. Strong bubble-emulsion phase mass transfer limitations would also explain the observed $CH_4$ conversion with the high applied space time of 99.2 $kg_{cat}{\cdot}s/mol_{CH4}$ fed, unless the catalyst is much less active than a conventional SMR catalyst as e.g. tested by Xu and Froment [1989].

Improving the bubble-emulsion phase mass transfer by increasing the gas velocity is challenging as particle entrainment is to be avoided. Increasing the particle size to allow higher fluidization gas velocities could be considered as long as intra-particle diffusion and heat transfer limitations remain negligible. In practice, however, it does not allow a sufficient increase of the gas

velocity, as the fraction of the bed occupied by bubbles becomes excessive because the bubble rise velocity does not increase proportionally with the gas flow rate.

## 7. CONCLUSIONS

Kinetic modelling requires identifying the relation between observed reaction rates and reaction conditions, that is, at the locus of reaction. This is in practice only possible under 'ideal' conditions, allowing the use of an as simple as possible reactor model as well. In that sense, a set of criteria is presented that can be used to verify to what extent the intrinsic kinetics of a heterogeneously catalyzed reaction can be measured in a bubbling fluidized bed under given operating conditions. The criteria ensure bubbling fluidization with a sufficiently small pressure drop and avoiding slugging and channelling. For the bubble phase, negligible axial dispersion is verified, whereas for the emulsion phase gas, negligible or dominant axial dispersion are considered. For reacting particles in the emulsion phase, complete mixing can be verified. Furthermore, it is verified if the radial temperature gradients are negligible and if segregation is avoided when applying bed dilution to ensure isothermal operation. Finally, it is verified if interfacial heat and mass transfer and intra-particle heat and mass transport limitations are negligible. For interfacial mass transfer limitations, bubble-emulsion phase mass transfer is considered on top of gas-solid heat and mass transfer.

A case study, considering the highly endothermic Steam Methane Reforming reaction, reveals that eliminating bubble-emulsion phase mass transfer limitations is particularly challenging. This is related to the superficial velocity range in which the bed can be operated. The relatively low superficial velocity also leads to a significant particle turnover time. Finally, preventing channelling requires generating a sufficiently high pressure drop over the gas distributor.

## ACKNOWLEDGEMENTS

The author would like to thank the Eurokin consortium for the financial support and Les Chewter (Shell Technology Centre Amsterdam) for the careful revision of this work. The author would like to

especially thank Prof. Guy Marin for the years of excellent guidance on the issues discussed in this paper and on kinetic and reactor modelling in general. And for the years of enjoyable discussions and friendship.

**NOTATIONS**

| | | |
|---|---|---|
| $A_o$ | Orifice area of the plate | $m^2$ |
| $Ar$ | Archimedes number, $\frac{\rho_f d_p^3(\rho_s-\rho_f)g}{\mu^2}$ | |
| $a$ | Dimensionless number, $\sqrt{1+4\beta\gamma r_{A0}}$ | |
| $a_g$ | Surface to volume ratio of a particle | $m_p^2/m_p^3$ |
| $Bi_w$ | Biot number, particle diameter based, $\frac{\alpha_w d_p}{\lambda_{er}}$ | |
| $\widetilde{Bi_w}$ | Biot number, tube diameter based, $\frac{\alpha_w d_t}{\lambda_{er}}$ | |
| $b$ | Bed diluation | $m_{inert}^3/m_s^3$ |
| $b_w$ | Weight fraction based bed dilution | $kg_{inert}^3/kg_s^3$ |
| $C_{Ae}$ | Molar concentration of A in the emulsion phase | $kmol/m_{eg}^3$ |
| $C_{Ab}$ | Molar concentration of A in the bubble phase | $kmol/m_b^3$ |
| $C_{A,b}$ | Bulk molar concentration of A | $kmol/m_g^3$ |
| $\Delta C_{A,fs}$ | Concentration difference between the solid surface and the bulk fluid | $kmol/m_g^3$ |
| $C_{A,s}^s$ | Molar concentration of A at the solid surface | $kmol/m_g^3$ |
| $C_{A0}$ | Molar feed concentration of A | $kmol/m_g^3$ |
| $C_D$ | Drag coefficient | |
| $c_{P,f}$ | Specific heat of fluid at constant pressure | $kJ/kg_f\,K$ |

| | | |
|---|---|---|
| $D_e$ | Axial diffusivity in the emulsion phase | $m_r^2/s$ |
| $D_{eA}$ | Effective diffusivity in a catalyst particle | $m_g^3/m_p\ s$ |
| $D'_{ea}$ | Effective axial diffusivity (superficial basis: $D'_{ea} = \varepsilon D_{ea}$) | $m_g^3/m_r\ s$ |
| $D'_{ea,b}$ | Effective axial diffusivity bubble phase (superficial basis) | $m_b^3/m_r\ s$ |
| $d_b$ | Bubble diameter | $m$ |
| $d_o$ | Orifice diameter | $m$ |
| $(d_p)_B$ | Particle diameter, big particles | $m_p$ |
| $d_p$ | Particle diameter | $m_p$ |
| $(d_p)_S$ | Particle diameter, small particles | $m_p$ |
| $d_t$ | Internal tube diameter | $m_r$ |
| $E$ | Activation energy | $kJ/mol$ |
| $F'$ | Volumetric flow rate | $m^3/s$ |
| $F_{Ae}$ | Molar feed rate in the emulsion phase | $kmol/s$ |
| $F_{g,or}$ | Volumetric flow rate of gas through an orifice | $cm^3/s$ |
| $f_b$ | Fraction of total fluidized bed volume occupied by bubble gas | $m_b^3/m_r^3$ |
| $f_e$ | Fraction of total fluidized bed volume occupied by emulsion gas | $m_{eg}^3/m_r^3$ |
| $G$ | Superficial fluid mass flux | $kg_f/m_r^2\ s$ |
| $g$ | Acceleration of gravity | $m/s^2$ |

| | | |
|---|---|---|
| $-\Delta H$ | Heat of reaction | $\mathrm{kJ/kmol}$ |
| $\mathrm{h}_f$ | Interphase gas-solid heat transfer coefficient | $\mathrm{kJ/m_p^2\ s\ K}$ |
| $J$ | Solids circulation flux | $\mathrm{kg_s/m_r^2\ s}$ |
| $j_D$ | j-factor for mass transfer | |
| $j_H$ | j-factor for heat transfer | |
| $k_I$ | Bubble-emulsion phase interchange coefficient | $\mathrm{m_g^3/m_r^3\ s}$ |
| $k_g$ | Mass transfer coefficient from gas to solid interface | $\mathrm{m_g^3/m_i^2\ s}$ |
| $L_o$ | Orifice length | $m$ |
| $L_{mf}$ | Fluidized bed height at minimum fluidization | $\mathrm{m_r}$ |
| $M_m$ | Mean molecular mass | $\mathrm{kg/kmol}$ |
| $N_o$ | Total number of orifices in the orifice plate | |
| $n$ | Reaction order | |
| $Pe_a$ | Peclet number based on particle diameter, $\frac{u_s d_p}{D_{ea}}$ | |
| $Pe'_a$ | Peclet number based on column length, $\frac{u_s Z}{D_{ea}}$ | |
| $Pe'_{a,b}$ | Bubble phase Peclet number based on column length, $\frac{f_b u_{br} Z}{D'_{ea,b}}$ or $\frac{u_{br} Z}{D_{ea,b}}$ | |
| $\mathrm{Pr}$ | Prandtl number, $\frac{c_p \mu}{\lambda}$ | |
| $\Delta p_b$ | Pressure drop through the bed | $\mathrm{N/m^2}$ |
| $\Delta p_d$ | Pressure drop through the distributor | $\mathrm{N/m^2}$ |
| $p_{fA}$ | Film pressure factor | $\mathrm{N/m^2}$ |
| $p_t$ | Total pressure | $\mathrm{N/m^2}$ |

| | | |
|---|---|---|
| $R$ | Gas constant | $\mathrm{kJ/kmol\ K}$ |
| $R_t$ | Tube radius | $\mathrm{m_r}$ |
| $\mathrm{Re}_{bf}$ | Reynolds number at beginning fluidization, $\frac{\rho_g u_{bf} d_p}{\mu}$ | |
| $\mathrm{Re}_{tf}$ | Reynolds number at total fluidization, $\frac{\rho_g u_{tf} d_p}{\mu}$ | |
| $\mathrm{Re}_p$ | Reynolds number, $\frac{\rho_g u_s d_p}{\mu}$ | |
| $RI_{im,r}$ | Maximum allowable relative influence of interphase mass transfer on the observed reaction rate | % |
| $r$ | Radial position inside the reactor | $\mathrm{m_r}$ |
| $r_A$ | Rate of reaction of component A per unit catalyst mass | $\mathrm{kmol/kg_{cat}.\ s}$ |
| $r_{A0}$ | Rate of reaction of component A per unit catalyst mass at the inlet | $\mathrm{kmol/kg_{cat}.\ s}$ |
| $r_p$ | Particle radius | $\mathrm{m_p}$ |
| $\Delta r_{rel}$ | Maximum acceptable relative difference between the observed and intrinsic reaction rates | % |
| $S_p$ | External particle surface area | $\mathrm{m_p^2}$ |
| $\mathrm{Sc}$ | Schmidt number, $\frac{\mu}{\rho_g \mathrm{D}}$ | |
| $T$ | Temperature | K |
| $T_B$ | Bulk / bed temperature | K |
| $\Delta T_{ad}$ | Adiabatic temperature difference through the reactor | K |

| | | |
|---|---|---|
| $\Delta T_{c,s}$ | Temperature difference between the solid centre and surface | K |
| $\Delta T_{c,w}$ | Temperature difference between the centre of the bed and the inner wall | K |
| $\Delta T_{s,f}$ | Temperature difference between the solid surface and the bulk fluid | K |
| $T_s$ | Temperature in the solid | K |
| $T_s^s$ | Temperature at the solid surface | K |
| $T_w$ | Inner reactor wall temperature | K |
| $t_T$ | Bed turnover time | s |
| $u_{br}$ | Bubble rise velocity | $m_r/s$ |
| $u_e$ | Emulsion gas velocity | $m_r/s$ |
| $u_{e,s}$ | Superficial emulsion gas velocity | $m_{eg}^3/m_r^2 s$ |
| $u_{bf}$ | Velocity at beginning fluidization | $m_g^3/m_r^2 s$ |
| $u_{i,fl}$ | Interstitial fluid velocity | $m_r/s$ |
| $u_{i,p}$ | Interstitial particle velocity | $m_r/s$ |
| $u_{mf}$ | Minimum fluidization velocity | $m_g^3/m_r^2 s$ |
| $(u_{mf})_F$ | Flotsam minimum fluidization velocity | $m_g^3/m_r^2 s$ |
| $u_s$ | Superficial gas velocity | $m_g^3/m_r^2 s$ |
| $u_t$ | Terminal or free-fall velocity | $m_r/s$ |
| $u_{tf}$ | Velocity at total fluidization | $m_g^3/m_r^2 s$ |
| $V_p$ | Particle volume | $m_p^3$ |

| | | |
|---|---|---|
| $V$ | Reactor volume | $\mathrm{m_r^3}$ |
| $w_i$ | Weight fraction particles of diameter $d_{pi}$ | |
| $x_A$ | Conversion of A | |
| $\Delta x_{rel}$ | Maximum acceptable relative deviation of the conversion | % |
| $y_{A0}$ | Mole fraction of A at the inlet | $\mathrm{mol_A/mol_f}$ |
| $Z$ | Column length / height | $\mathrm{m_r}$ |
| $z$ | Axial position inside the reactor | $\mathrm{m_r}$ |
| $\alpha_w$ | Convective heat transfer coefficient in the vicinity of the wall | $\mathrm{kJ/m^2\ s\ K}$ |
| $\beta$ | Dimensionless number, $\frac{\rho_e(1-f_b)Z}{u_e f_e C_{A0}}$ | |
| $\gamma$ | Dimensionless number, $\frac{D_e}{u_e Z}$ | |
| $\epsilon_p$ | Emissivity of the particles | |
| $\epsilon_s$ | Emissivity of the heat exchange surface | |
| $\varepsilon$ | Gas holdup | $\mathrm{m_g^3/m_r^3}$ |
| $\varepsilon_e$ | Emulsion phase void fraction | $\mathrm{m_{eg}^3/m_e^3}$ |
| $\varepsilon_{mf}$ | Void fraction at minimum fluidization | $\mathrm{m_g^3/m_r^3}$ |
| $\lambda_b^0$ | Static contribution thermal conductivity of the (fixed) bed | $\mathrm{kJ/m_r\ s\ K}$ |
| $\lambda_e$ | Effective thermal conductivity in a solid particle | $\mathrm{kJ/m_p\ s\ K}$ |
| $\lambda_{er}$ | Effective thermal conductivity in the radial direction | $\mathrm{kJ/m_r\ s\ K}$ |
| $\lambda_g$ | Gas thermal conductivity | $\mathrm{kJ/m_g\ s\ K}$ |

| | | |
|---|---|---|
| $\mu$ | Gas viscosity | kg/m s |
| $\rho_B$ | Catalyst bulk density | $\mathrm{kg_{cat}/m_r^3}$ |
| $\rho_b$ | Bulk density of bubble phase | $\mathrm{kg_{cat}/m_b^3}$ |
| $\rho_e$ | Bulk density of emulsion phase | $\mathrm{kg_{cat}/m_e^3}$ |
| $\rho_g$ | Gas density | $\mathrm{kg_g/m_g^3}$ |
| $\rho_s$ | Solid density | $\mathrm{kg_p/m_p^3}$ or $\mathrm{kg_{cat}/m_{cat}^3}$ |
| $(\rho_s)_{F/J}$ | Solid density of flotsam (F) / jetsam (J) particles | kg F/J particles/$\left(\mathrm{m_p^3}\right)_{\mathrm{F/J}}$ |
| $\Omega$ | Reactor cross section | $\mathrm{m_r^2}$ |

**REFERENCES**


Abrahamsen AR, Geldart D. Behaviour of gas-fluidized beds of fine powders part I. Homogeneous expansion. Powder Technol. 26(35):35-46, 1980.

Abrahamsen AR, Geldart D. Behaviour of gas-fluidized beds of fine powders part II. Voidage of the dense phase in bubbling beds. Powder Technol. 26(35):47-55, 1980.

Abrahamsen AR, Geldart D. Behaviour of gas-fluidized beds of fine powders part III. Effective thermal conductivity of a homogeneously expanded bed. Powder Technol. 26(35):57-65, 1980.

Agarwal PK, La Nauze RD. Transfer processes local to the coal particle: a review of drying, devolatilization and mass transfer in fluidized bed combustion. Chem. Eng. Res. Des. 67:457-480, 1989.

Agu CE, Tokheim L-A, Eikeland M, Moldestad BME. Improved models for predicting bubble velocity, bubble frequency and bed expansion in a bubbling fluidized bed. Chem. Eng. Res. Des. 141:361-371, 2019.

Anderson JB. A criterion for isothermal behaviour of a catalyst pellet. Chem. Eng. Sci. 18:147, 1963.

Avedesian MM. Combustion of char in fluidized beds. PhD dissertation: University of Cambridge, 1972.

Baeyens J, Geldart D. Fluidization et ses Applications. Toulouse, 182, 1973.

Baeyens J, Geldart D. An investigation into slugging fluidized beds. Chem. Eng. Sci. 29:255-265, 1974.

Baird MHI, Rice RG. Axial dispersion in large unbaffled columns. Chem. Eng. J. 9:171-174, 1975.

Balakrishnan AR, Pei DCT. Fluid particle heat transfer in gas fluidized beds. Can. J. Chem. Eng. 53:231-233, 1975.

Baskakov AP. Heat transfer in fluidized beds: Radiative heat transfer in fluidized beds. In: Davidson JF, Harrison D, eds. Fluidization, 2nd ed. London: Academic Press, 465-472, 1985.

Baskakov AP, Berg BV, Vitt OK, Filippovsky NF, Kirakosyan VA, Goldobin JM, Maskaev VK. Heat Transfer to Objects Immersed in Fluidized Beds. Powder Technol. 8(5-6):273-282, 1973; In: Fluidization and Its Applications. p. 293, Cepadues, Toulouse, 1974.

Baskakov AP, Vitt OK, Kirakosyan VA, Maskaev VK, Filippovsky NF. Investigation of Heat Transfer Coefficient Pulsations and of the Mechanism of Heat Transfer from a Surface Immersed Into a Fluidised Bed. International Symposium Fluidization Applications, France, 1974.

Behie LA, Bergougnou MA, Baker CGJ, Bulani W. Jet momentum dissipation at a grid of a large gas fluidized bed. Can. J. Chem. Eng. 48:158-161, 1970.

Behie LA, Bergougnou MA, Baker CGJ. Heat transfer from a grid jet in a large fluidized bed. Can. J. Chem. Eng. 53:25-30, 1975.

Behie LA, Bergougnou MA, Baker CGJ. Mass transfer from a grid jet in a large gas fluidized bed. In: Keairns DL, ed. Fluidization Technology, Vol 1. Washington DC: Hemisphere, 261-278, 1976.

Berger RJ, Pérez-Ramirez J, Kapteijn F, Moulijn JA. Catalyst Performance Testing: Bed Dilution Revisited. Chem. Eng. Sci. 57(22):4921-4932, 2002.

Beyke CJ, "Characteristics of a stirred bed reactor used for gas-solid reactions". Masters Theses. 318, 1986. https://scholarsmine.mst.edu/masters_theses/318

Carberry JJ. Chemical and Catalytic Reaction Engineering. McGraw-Hill, New York, 1976.

Carberry JJ, Wendel M. A computer model of the fixed bed catalytic reactor: The adiabatic and quasi-adiabatic cases. AIChE J. 9(1):129-133, 1963.

Chambré PL, Grossman LM. On limiting temperatures in chemical reactors. Appl. Sci. Res. Sec. A, 5:245-254, 1955.

Chen JLP, Keairns DL. Particle segregation in a fluidized bed. Can. J. Chem. Eng. 53:395-402, 1975.

Chen H, Zheng Z, Shi W. Investigation on the Kinetics of Iron Ore Fines Reduction by CO in a Micro-fluidized Bed. Procedia Engineering 102:1726-1735, 2015.

Chen H, Zheng Z, Chen Z, Bi XT. Reduction of hematite (Fe2O3) to metallic iron (Fe) by CO in a micro fluidized bed reaction analyser: A multistep kinetics study. Powder Technology 316:410-420, 2017.

Chen H, Zheng Z, Chen Z, Yu W, Yue J. Multistep Reduction Kinetics of Fine Iron Ore with Carbon Monoxide in a Micro Fluidized Bed Reaction Analyzer. Metallurgical and Materials Transactions B 48B:841-852, 2017b.

Chen K, Zhao Y, Zhang W, Feng D, Sun S. The intrinsic kinetics of methane steam reforming over a nickel-based catalyst in a micro fluidized bed reaction system. International Journal of Hydrogen Energy 45:1615-1628, 2020.

Chiba S, Nienow AW, Chiba T, Kobayashi H. Fluidized binary mixtures in which the dense component may be flotsam. Powder Technol. 26:1-10, 1980.

Cocco R, Karri SBR, Knowlton T. Introduction to fluidization. AIChE Journal 1-9, 2014.

Couwenberg PM, Chen Q, Marin GB. Irreducible mass-transport limitations during a heterogeneously catalyzed gas-phase chain reaction: The oxidative coupling of methane. Industrial & Engineering Chemistry Research, 35, 415-421, 1996.

Darton RC, La Nauze RD, Davidson JF, Harrison D. Bubble growth due to coalescence in fluidized beds. Trans. Inst. Chem. Eng. 55:274-280, 1977.

Davidson JF, Harrison D. Fluidised Particles. London: Cambridge University Press, 1963.

Davidson JF, Schuler BOG. Bubble formation at an orifice in an inviscid liquid. Trans. Inst. Chem. Eng. 38:335-342, 1960.

De Wilde J, Das AK, Heynderickx GH, Marin GB. Development of a transient kinetic model for the simultaneous adsorption of $SO_2$-NOx over Na/γ-$Al_2O_3$ sorbent. Industrial & Engineering Chemistry Research 40:1, 119-130, 2001.

Dow WM, Jakob M. Heat transfer between a vertical tube and a fluidized air-solid flow. Chem. Eng. Progress. Symp. Series 637-648, 1951.

Field RW, Davidson JF. Axial dispersion in bubble columns. Trans. Inst. Chem. Engrs. 58:228-236, 1980.

Froment G.F., Bischoff K.B., De Wilde J., Chemical Reactor Analysis and Design, 3th ed., Wiley, 2010.

Frössling N. The evaporation of falling drops (in German: Uber die Verdunstung Fallender Tropfen). Gerlands Beiträge zur Geophysik, 52:170-216, 1938.

Gao W, Farahani MR, Rezaei M, Qudair Baig A, Jamil MK, Imran M, Rezaee-Manesh R. Kinetic modelling of biomass gasification in a micro fluidized bed. Energy Sources, Part A: Recovery, Utilization and Environmental Effects 39(7):643-648, 2017.

Geldart D. Gas Fluidization Technology. Chichester, John Wiley, 1986.

Geldart D. Types of gas fluidization. Powder Technology 7(5):285-292, 1973.

Geldart D, Abrahamsen AR. Homogeneous fluidization of fine powders using various gases and pressures. Powder Technol. 19:133-136, 1978.

Gelperin NI, Einstein VG, Nosov GA, Mamoshkina VV, Rebrova SK. Teor Osnovy Khim Tehnol. 1:383, 1967.

Gierman H. Design of laboratory hydrotreating reactors – Sacling down of trickle-flow reactors. Appl. Catal. 43: 277-286, 1988.

Glicksman LR, Decker N. Heat Transfer in Fluidized Beds of Large Particles. Report from Mech. Eng. Dept., M.I.T., Cambridge, MA, USA, 1983.

Guo Y, Zhao Y, Meng S, Feng D, Yan T, Wang P, Sun S. Development of a Multistage in Situ Reaction Analyzer Based on a Micro Fluidized Bed and its Suitability for Rapid Gas-Solid Reactions. Energy Fuels 30:6021-6033, 2016.

Guo Y, Zhao Y, Gao D, Liu P, Meng S, Sun S. Kinetics of steam gasification of in-situ chars in a micro fluidized bed. International Journal of Hydrogen Energy 41:15187-15198, 2016b.

Gupta AS, Thodos G. Direct Analogy Between Mass and Heat Transfer to Beds of Spheres. AIChE J. 9(6):751-754, 1963.

Gupta SN, Chaube RB, Upadhyay. Fluid-particle heat transfer in fixed and fluidized beds. Chem. Eng. Sci. 29(3):839-843, 1974.

Haider A, Levenspiel O. Powder Technol., 58:63, 1989.

Harrison D, Leung LS. Bubble formation at an orifice in a fluidized bed. Nature, 190:433-434, 1961.

Hiby JW. Critical minimum pressure drop of gas distribution plate in fluidized bed units. Chem. Ing. Tech. 36:228, 1964.

Hilligardt K, Werther J. in Proc. 3rd World Cong. Chem. Eng., Tokyo, 1986.

Hsiung TH, Thodos G. Mass transfer in gas-fluidized beds: measurement of actual driving forces. Chem. Eng. Sci. 32:581-592, 1977.

Joshi JB. Axial mixing in multiphase contactors – a unified correlation. Trans. Inst. Chem. Engs. 58:228-236, 1980.

Joshi JB. Gas phase dispersion in bubble columns. Chem. Eng. J. 24:213–216, 1982.

Karri SR, Knowlton T. Gas Distributior and Plenum Design in Fluidized Beds. Fluidization Solids Handling and Processing 1:209–235, 1999.

Karri SBR, Knowlton TM. A comparison of annulus solids flow direction and radial solids mass flux profiles at low and high mass fluxes in a riser. In: Werther J, ed. Circulating Fluidized Bed Technology VI. Frankfurt: DECHEMA, p. 71-76, 1999.

Kok J, Stark NL, van Swaaij WPM. In: Ostergaard K, Soorensen A, eds. Fluidization V, Elsionore, Denmark. New York: Engineering Foundation, 1986.

Kondukov NB, Sosna MH. Khim Prom 6:402, 1965.

Kothari AK, Analysis of Fluid-Solid Heat Transfer Coefficients in Fluidized Beds, M.S. Thesis, Illinois Institute of Technology, Chicago, 1967.

Kumar A, Sen Gupta P. Prediction of minimum fluidization velocity for multi-component mixtures. Indian J. Technol. 12:225-228, 1974.

Kunii D, Levenspiel O. Fluidization Engineering. 1st ed. New York: John Wiley, 1969.

Kunii D, Levenspiel O. Fluidization Engineering. 2nd ed. Boston: Butterwworth-Heinemann, 1991.

Lee A, Miller DC. A One-Dimensional (1-D) Three-Region Model for a Bubbling Fluidized-Bed Adsorber. Ind. Eng. Chem. Res. 52:469-484, 2013.

Leva M. Fluidization. McGraw-Hill, New York, 1960.

Levenspiel O, Walton JS. Bed wall heat transfer in fluidized system. Chem. Eng. Progr. Symp. Series 9:1-13, 1954.

Li Y., Li Z., Wang H., Cai N., CaO carbonation kinetics determined using micro-fluidized bed thermogravimetric analysis. Fuel, 264(1), 116823, 2020.

Linjewile TM, Agarwal PK. The 23rd Symposium on Combustion. Combustion Inst., 917, 1990.

Mears DE. Diagnostic criteria for heat transport limitations in fixed bed reactors. J. Catal. 20(2):127-131, 1971.

Mears DE. Ind. Eng. Chem. Proc. Des. Dev. 10 :541, 1971b.

Mears DE. Role of axial dispersion in trickle-flow laboratory reactors. Chem. Eng. Sci. 26:1361-1366, 1971c.

Medrano JA, Gallucci F, Boccia F, Alfano N, van Sint Annaland M. Determination of the bubble-to-emulsion phase mass transfer coefficient in gas-solid fluidized beds using a non-invasive infra-red technique. Chem. Eng. J., 325:404-414, 2017a.

Medrano JA, Tasdemir M, Gallucci F, van Sint Annaland M. On the internal solids circulation rates in freely-bubbling gas-solid fluidized beds. Chem. Eng. Sci., 172:395-406, 2017b.

Mickley HS, Fairbanks DE, Hautorn RD. The relation between the transfer coefficient and thermal fluctuations in fluidized-bed heat transfer. Chem. Eng. Progr. Symp. Series 32:51-60, 1961.

Mickley HS, Fairbanks DE. Mechanism of heat transfer to fluidized beds. AIChE Journal 9:374-348, 1955.

Minette F, Lugo-Pimentel M, Modroukas D, Davis AW, Gill R, Castaldi MJ, De Wilde J. Intrinsic kinetics of steam methane reforming on a thin, nanostructured and adherent Ni coating. Appl. Catal. B: Environ. 238:184-197, 2018.

Mireur JP, Bischoff KB. Mixing and contacting models for fluidized beds. AIChE Journal 13(5):839-845, 1967.

Mori S, Moriyama A. Criteria for uniform fluidization of non-aggregative particles. Int. Chem. Eng. 18:245-249, 1978.

Oka S. Fluidized Bed Combustion, Fundamentals and Application. Beograd, Yugoslav Society of Thermal Engineers (ed.), 1994.

Palchonok GI, Tamarin AI. Mass transfer at a moving particle in a fluidized bed of coarse material. J. Eng. Phys. 47:916-922, 1984.

Palchonok GI, Dolidovich AF, Andersson S, Leckner B. Calculation of true heat and mass transfer coefficients between particles and a fluidized bed. In: Potter OE, Nicklin DJ, eds. Fluidization VII, Brisbane, Australia. New York: Engineering Foundation, 913-920, 1992.

Perry RH, Green DW, Maloney JO. Perry's Chemical Engineers' Handbook. 6$^{th}$ ed. McGraw-Hill, New York, 1984.

Pielsticker S, Gövert B, Kreitzberg T, Habermehl M. Development of a rapidly responding fluidized bed reactor by theoretical and experimental evaluation of combustion reactions. Fuel 223(2):462-469, 2018.

Pillai KK. The effective radial conductivity of fluidized beds. J. Inst. of Energy 419:100-102, 1981.

Prins W, Casteleijn TP, Draijer W, van Swaaij WPM. Mass transfer from a freely moving single sphere to the dense phase of a gas fluidized bed of inert particles. Chem. Eng. Sci. 40(3):481-497, 1985.

Resnick WE, White RR. Mass transfer in systems of gas and fluidized solids. Chem. Eng. Prog. 45:377-390, 1949.

Rowe PN, Nienow AW, Agbim AJ. A preliminary quantitative study of particle segregation in gas fluidized beds binary systems of near spherical particles. Trans. Inst. Chem. Eng. 50:324-33, 1972.

Scala F. Mass transfer around freely moving active particles in the dense phase of a gas fluidized bed of inert particles. Chem. Eng. Sci. 62:4159-4176, 2007.

Shi YF, Fan LT. Lateral mixing of solids in batch gas-solids fluidized beds. Ind. Eng. Chem. Process. Des. Dev. 23:337-341, 1984.

Siegel R. Effect of distributor plate-to-bed resistance ratio on onset of fluidized-bed channeling. AIChE J. 22(3):590-592, 1976.

Stewart PSB. PhD dissertation. Cambridge Univ., 1965.

Stewart PSB, Davidson JF. Slug flow in fluidized beds. Powder Tech. 1:61-80, 1967.

Toomey RD, Johnstone HF. Heat transfer between beds of fluidized solids and the walls of the container. Chem. Eng. Progr. Symp. Series 5:51-63, 1953.

Towell GD, Ackerman GH, Eur. Symp. On Chemical Reaction Engineering, 5$^{th}$ Amsterdam, Elsevier, 1972.

Trambouze P, Van Landeghem H, Waucquier JP. Les Réacteurs Chimiques. Eds. Technip, Paris, 1984.

Vaid RP, Sen Gupta P. Minimum fluidization velocities in beds of mixed solids. Can. J. Chem. Eng. 56:292-296, 1978.

van Heerden C, Nobel APP, van Krevelen DW. Mechanism of heat transfer in fluidized beds. Ind. Eng. Chem. 6:1237-1242, 1953.

van Swaaij WPM, Zuiderweg FJ. Investigation of ozone decomposition in fluidized beds on the basis of a two-phase model. Proc. 5th Eur./2nd Int. Symp. Chem. React. Eng., Elsevier, Amsterdam, p. B-9-25, 1972.

Vandershuren I, Delvosalle C. Particle-to-particle heat transfer in fluidized bed drying. Chem. Eng. Sci. 35:1741-1748, 1980.

Vandewalle LA, Van Geem KM, Marin GB, Bos R. A Boudart number for the assessment of irreducible pellet-scale mass transfer limitations: Application to oxidative coupling of methane. Industrial & Engineering Chemistry Research 60:18, 6538-6553, 2021.

Wehner JF, Wilhelm RH. Boundary conditions of flow reactor. Chem. Eng. Sci. 6(2):89-93, 1956.

Weisz PB, Prater CD. Interpretation of Measurements in Experimental Catalysis. Adv. Catal. 6:143-196, 1954.

Wen Cy, Leva M. Fluidized-bed heat transfer. A generalized dense-phase correlation. AIChE Journal 3:482-488, 1956.

Wender L, Cooper GT. Heat transfer between fluidized-solids beds and boundary surfaces – Correlation of data. AIChE Journal 1:15-23, 1958.

Werther J. in *Fluidization*, Davidson J.F. and Keairns D.L., eds., Cambridge Univ. Press, New York, 7, 1978.

Werther J, Hartge E-U. Modelling of Fluidized Bed Reactors. Int. J. Chem. React. Eng. 1(1), 2003.

Werther J. Bubble growth in large diameter fluidized beds. In: Keairns DL, ed. Fluidization Technology. Washington: Hemisphere 215-235, 1976a.

Werther J. Convective solids transport in large diameter gas fluidized beds. Powder Technol. 15:155-167, 1976b.

Xu J, Froment GF. Methane Steam Reforming, Methanation and Water-Gas Shift: I. Intrinsic Kinetics. AIChE J. 35: 88-96, 1989.

Yang WC. Bubbling fluidized beds. In: Handbook of Fluidization and Fluid–Particle System, 2003.

Young LC, Finlayson BA. Axial dispersion in nonisothermal packed bed chemical reactors. Ind. Eng. Chem. Fundam. 12(4):412-422, 1973.

Zenz F, Othmer DF. Fluidization and Fluid-Particle Systems. New York: Reinhold, 1960.

Zhang Y, Yao M, Sun G, Gao S, Xu G. Characteristics and Kinetics of Coked Catalyst Regeneration via Steam Gasification in a Micro Fluidized Bed. Industrial & Engineering Chemistry Research 53:6316-6324, 2014.

Zhang Y, Sun G, Gao S, Xu G. Regeneration Kinetics of Spent FCC Catalyst via Coke Gasification in a Micro Fluidized Bed. 102:1758-1765, 2015.

Zhang Y, Yao M, Gao S, Sun G, Xu G. Reactivity and kinetics for steam gasification of petroleum coke blended with black liquor in a micro fluidized bed. Applied Energy 160:820-828, 2015.

Zuiderweg FJ. In Proc. Intern. Symp. On Fluidization, A.A.H. Drinkenburg, ed., Netherlands Univ. Press, Amsterdam, 739, 1967.

**TABLES AND FIGURES**

| | | | |
|---|---|---|---|
| SLUGGING AVOIDED | | | |
| Orifice plate distributor – criterion Eq. (6) | | | |
| $d_b(Z)$ – Eq. (4) | < ? | $d_t$ | Satisfied |
| $1.52 \cdot 10^{-2}\ [m]$ | | $2 \cdot 10^{-2}\ [m]$ | |
| Porous plate distributor – criterion Eq. (6) | | | |
| $d_b(Z)$ – Eq. (5) | < ? | $d_t$ | Satisfied |
| $1.99 \cdot 10^{-2}\ [m]$ | | $2 \cdot 10^{-2}\ [m]$ | |
| Alt. criterion Eq. (11) | | | |
| $u_{b,ms}$ – Eq. (9) / (12) | > ? | $u_{br}$ – Eqs. (97)-(98) | Satisfied |
| $5.20 \cdot 10^{-3}\ [m_r/s]$ / $9.55 \cdot 10^{-2}\ [m_r/s]$ | | $1.00 \cdot 10^{-1}\ [m_r/s]$ | |
| OR: $z_s$ – Eq. (10) | > ? | $Z$ | |
| $6.77 \cdot 10^{-1}\ [m_r]$ | | $1.01 \cdot 10^{-1}\ [m_r]$ | |
| CHANNELLING AVOIDED | | | |
| Criterion Eq. (15) or more severe Eq. (16) ($Z$ < 0.3 m) | | | |
| $\Delta p_d$ – Eq. (22) | ≥ ? | $\Delta p_b$ – Eq. (50) | Satisfied |
| $6.24 \cdot 10^{2}\ [Pa]$ | | $6.12 \cdot 10^{2}\ [Pa]$ | |
| Alt. criterion Eq. (17) | | | |
| Porous plate | | | |
| $\frac{\Delta p_d}{\Delta p_b}$ – Eqs. (22) & (50) | ≥ ? | $\left(\frac{L_f}{L_{mf}} - 1\right)\frac{1}{1-(u_{mf}/u_s)}$ – Eq. (83) / (84) | Satisfied |
| 1.02 | | $5.72 \cdot 10^{-1}$ | |
| Perforated plate | | | |
| $\frac{\Delta p_d}{\Delta p_b}$ – Eqs. (22) & (50) | ≥ ? | $\left(\frac{L_f}{L_{mf}} - 1\right)\frac{1}{1-(u_{mf}/u_s)^2}$ – Eq. (83) / (84) | Satisfied |
| 1.02 | | $5.07 \cdot 10^{-1}$ | |
| ISOBARIC OPERATION | | | |
| Criterion Eq. (49) | | | |
| $\Delta p_b$ – Eq. (50) | < ? | $0.2\frac{p_t}{n}$ | Satisfied |
| $6.12 \cdot 10^{2}\ [Pa]$ | | $4.00 \cdot 10^{4}\ [Pa]$ | |
| AXIAL DISPERSION | | | |
| BUBBLE PHASE – NEGLIGIBLE EFFECT AXIAL DISPERSION | | | |
| Criterion Eq. (25) | | | |
| $Pe'_{a,b}$ – Eq. (26) | ≫ ? | 1 | Satisfied |
| $3.91 \cdot 10^{1}$ | | | |
| $Pe'_{a,b}$ – Eq. (27) | ≫ ? | 1 | Satisfied |
| $2.28 \cdot 10^{1}$ | | | |
| EMULSION PHASE – (a) OR (b) | | | |
| (a) NEGLIGIBLE EFFECT AXIAL DISPERSION – CRITERION EQ. (39) | | | |
| $Pe_{a,eg}$ – Eq. (39) | >> ? | $\frac{\rho_e(1-f_b)r_{A0}d_p}{u_e f_e C_{A0}}$ – Eqs. (96) & (99) | Not satisfied |
| $1.19 \cdot 10^{-5}$ | | $1.46 \cdot 10^{-2}$ | |
| (b) DOMINANT AXIAL DISPERSION – CRITERION EQ. (43) | | | |
| $\left\|\frac{x_{Ae1}(1) - x_{Ae1}(0)}{x_{Ae1}(1)}\right\|$ – Eq. (32), (33) & (43) | < ? | $\Delta r_{rel}$ (max allowable error) | Satisfied |
| $2.85 \cdot 10^{-2}$ | | 0.05 | |

**Table 1.** Criteria verification for the case of Steam Methane Reforming at 500°C.

| ISOTHERMAL OPERATION | | | |
|---|---|---|---|
| NEGLIGIBLE RADIAL TEMPERATURE GRADIENT – CRITERION EQ. (52) OR EQ. (53)/(54) | | | |
| $\Delta T_{c,w}$ – Eq. (52) or (53)/(54) & Eq. (113) or (116) | < ? | $\Delta r_{rel}\frac{2RT_w^2}{E}$ | Satisfied |
| $8.09 \cdot 10^{-2}\ [K]$ | | $2.35\ [K]$ (with $\Delta r_{rel} = 0.05$) | |
| ACCEPTABLE BED DILUTION – CRITERION EQ. (55) | | | |
| $b$ | < ? | $\frac{\Delta x_{rel}}{\Delta x_{rel} + \frac{0.5 n x_A d_p}{L}}$ | Satisfied |
| 0.850 | | 0.99596 | |

| NEGLIGIBLE BUBBLE-EMULSION PHASE MASS TRANSFER LIMITATIONS – (a) OR (b) | | | |
|---|---|---|---|
| (a) PLUG FLOW BUBBLE PHASE AND EMULSION GAS – CRITERION EQ. (69) | | | |
| $\frac{n r_A(C_{A0})\rho_e(1-f_b)}{2k_I C_{A0}}$ – Eqs. (96) & (117) | < ? | $RI_{im,r}$ | Not satisfied (and criterion not applicable as emulsion gas well-mixed) |
| $2.38 \cdot 10^{-1}$ | | 0.05 (max allowable % error) | |
| (b) PLUG FLOW BUBBLE PHASE AND WELL-MIXED EMULSION GAS – CRITERION EQ. (77) | | | |
| $\left\lvert \frac{-n r_A(\overline{C_A})\rho_e(1-f_b)}{2k_I\left[C_{A0} - r_A(\overline{C_A})\frac{\rho_e(1-f_b)Z}{f_b u_b + f_e u_e}\right]} \right\rvert$ – Eqs. (96), (99) & (117) | < ? | $RI_{im,r}$ | Not satisfied |
| $1.97 \cdot 10^{-1}$ | | 0.05 (max allowable % error) | |

| NEGLIGIBLE GAS-SOLID HEAT TRANSFER LIMITATIONS – CRITERION EQ. (78) | | | |
|---|---|---|---|
| Using Eq. (126) for $j_H$ | | | |
| $\Delta T_{s,f}$ – Eqs. (78), (122) & (126) | < ? | $\Delta r_{rel}\frac{RT_B^2}{E}$ | Satisfied |
| $0.04\ [K]$ | | $1.03\ [K]$ (with $\Delta r_{rel} = 0.05$) | |
| Using Eq. (127) for $j_H$ | | | |
| $\Delta T_{s,f}$ – Eqs. (78), (122) & (127) | < ? | $\Delta r_{rel}\frac{RT_B^2}{E}$ | Satisfied |
| $0.65\ [K]$ | | $1.03\ [K]$ (with $\Delta r_{rel} = 0.05$) | |

| NEGLIGIBLE GAS-SOLID MASS TRANSFER LIMITATIONS – CRITERION EQ. (79) | | | |
|---|---|---|---|
| Using Eq. (140) for $k_g$ | | | |
| $\Delta C_{A,fs}$ – Eqs. (79), (131) & (140) | < ? | $RI_{im,r}\frac{C_{A,e}}{n}$ | Satisfied |
| $2.71 \cdot 10^{-6}\ [kmol/m_f^3]$ | | $1.55 \cdot 10^{-4}\ [kmol/m_f^3]$ (with $RI_{im,r} = 0.05$) | |

| NEGLIGIBLE INTRA-PARTICLE HEAT TRANSPORT LIMITATIONS – CRITERION EQ. (80) | | | |
|---|---|---|---|
| $\Delta T_{c,s}$ – Eq. (80) | < ? | $\Delta r_{rel}\frac{5RT_s^{s^2}}{2E}$ | Satisfied |
| $1.0 \cdot 10^{-2}\ [K]$ | | $2.59\ [K]$ (with $\Delta r_{rel} = 0.05$) | |
| NEGLIGIBLE INTRA-PARTICLE DIFFUSION LIMITATIONS – CRITERION EQ. (81) / (82) | | | |
| $\frac{(n+1)\overline{r_A}\rho_s}{2a_g^2 D_{eA} C_{A,s}^s}$ | < ? | 0.33 for n = 0<br>0.08 for n ≥ 0.5 | Satisfied |
| $8.41 \cdot 10^{-4}$ | | | |

**Table 1-continued.** Criteria verification for the case of Steam Methane Reforming at 500°C.

| PARTICLE MIXING | |
|---|---|
| Solids circulation flux $J$ – Eq. (45) | $6.48\ [kg/m_r^2 s]$ |
| Bubble shape factor<br>$\phi_b$ – Eq. (46)<br>$\omega$ – Eq. (47) | <br>$7.62 \cdot 10^{-1}$<br>$2.09 \cdot 10^{-1}$ |
| Turnover time $t_T$ – Eq. (48) | $9.63\ [s]$ |

**Table 2.** Particle mixing characteristics.

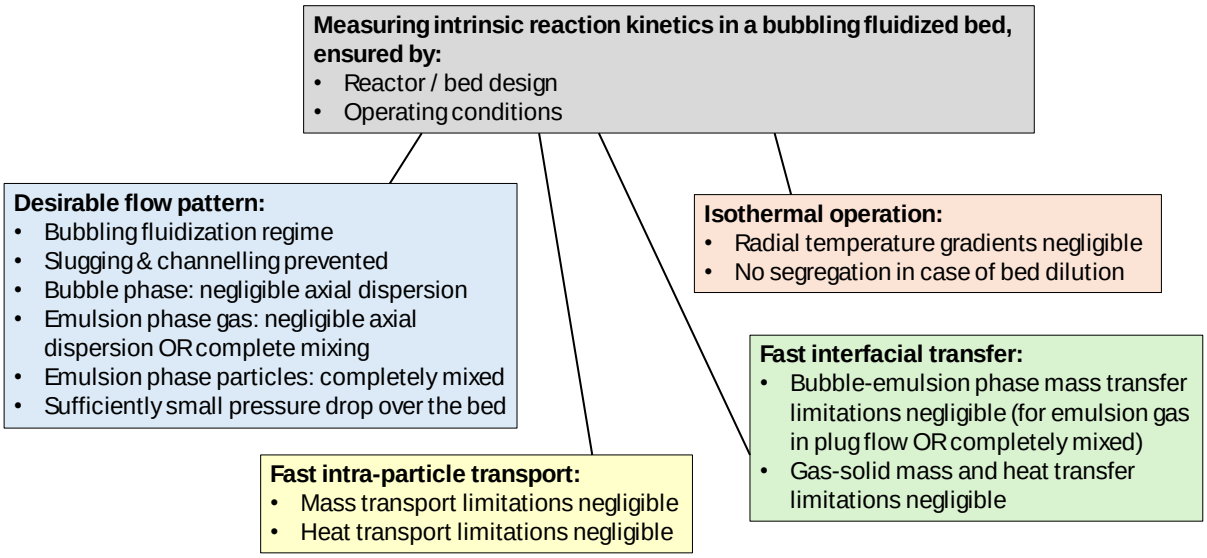


**Figure 1.** Different aspects to be dealt with when aiming at measuring intrinsic reaction kinetics in a bubbling fluidized bed.

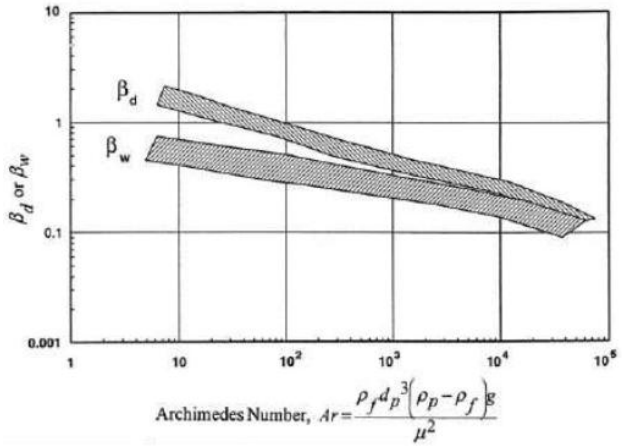


| Powder | Size (μm) | $\beta_w$ | $\beta_d$ | $Y$ |
|---|---|---|---|---|
| Catalyst | 47 | 0.43 | 1.00 | 1.00 |
| Angular sand | 252 | 0.26 | 0.42 | 0.50 |
| | 470 | 0.20 | 0.28 | 0.25 |
| Round sand | 106 | 0.32 | 0.70 | 0.82 |
| | 195 | 0.30 | 0.52 | 0.65 |

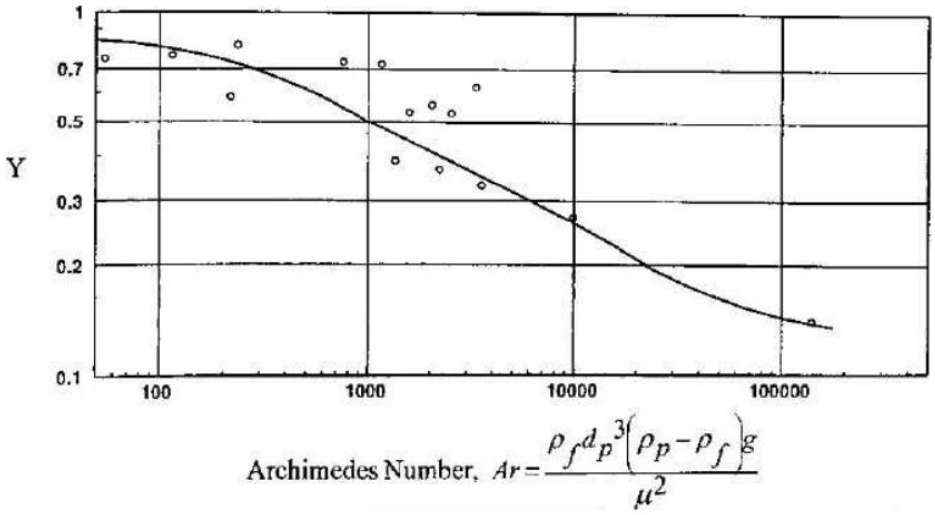


**Figure 2.** Wake and drift fraction and correction for deviation from the two-phase theory as in Eq. (44) vs. particle characteristics and tabulated values for some commonly used materials. Adapted from Geldart [1986] and Baeyens and Geldart [1973], from Yang [2003].

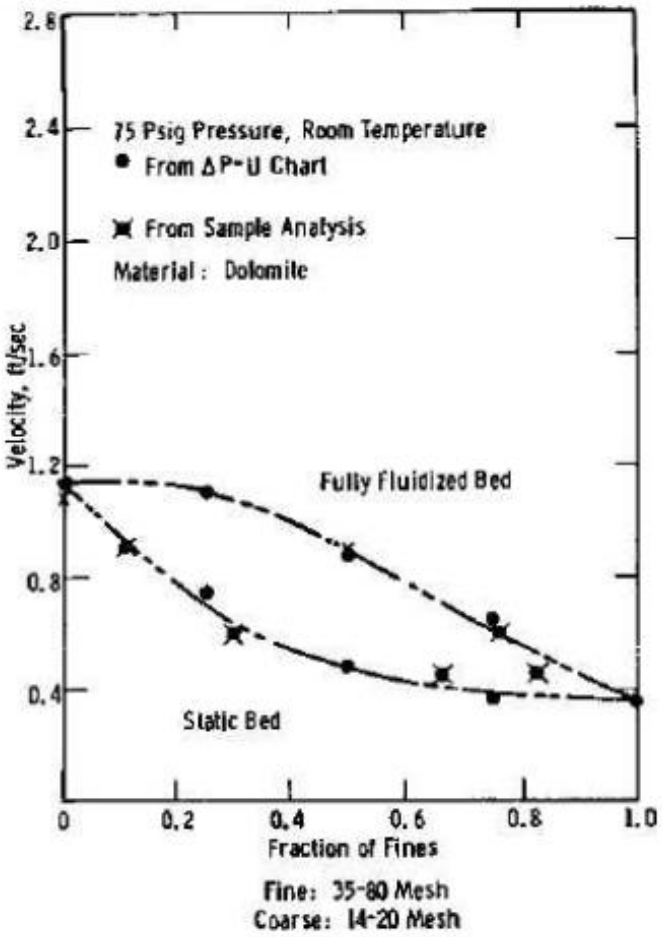


**Figure 3.** Phase equilibrium type diagram for a bed containing fine and coarse particles, illustrating beginning fluidization and total fluidization [Yang, 2003; Adapted from Chen and Keairns, 1975].

| | | |
|---|---|---|
| Case I | $d_B/d_S \leq 10$ | |
| $I_a$ | $\rho_B = \rho_S$ | Jetsam = bigger component |
| $I_b$ | $\rho_B \neq \rho_S$ | Jetsam = heavier component |
| Case II | $d_B \gg d_S$ and bed material $\rightarrow$ 100% smaller component | |
| $II_a$ | $\rho_B > (\rho_B)_S$ | Jetsam = bigger component |
| $II_b$ | $\rho_B < (\rho_B)_S$ | Jetsam = smaller component |
| Case III | $d_B \gg d_S$ and bed material $\rightarrow$ 100% bigger component | |
| $III_a$ | $\rho_B > \rho_S$ | Jetsam = bigger component |
| $III_b$ | $\rho_B < \rho_S$ | Jetsam = either component may be jetsam |
| Case IV | The minor component is platelike with $\phi < 0.5$ | |
| $IV_a$ | Platelike particle is denser | Jetsam = platelike component |
| $IV_b$ | Platelike particle is lighter | Jetsam = either component may be jetsam |

**Figure 4.** Flotsam-Jetsam classification for a binary particle bed [Chiba et al., 1980; Yang, 2003].

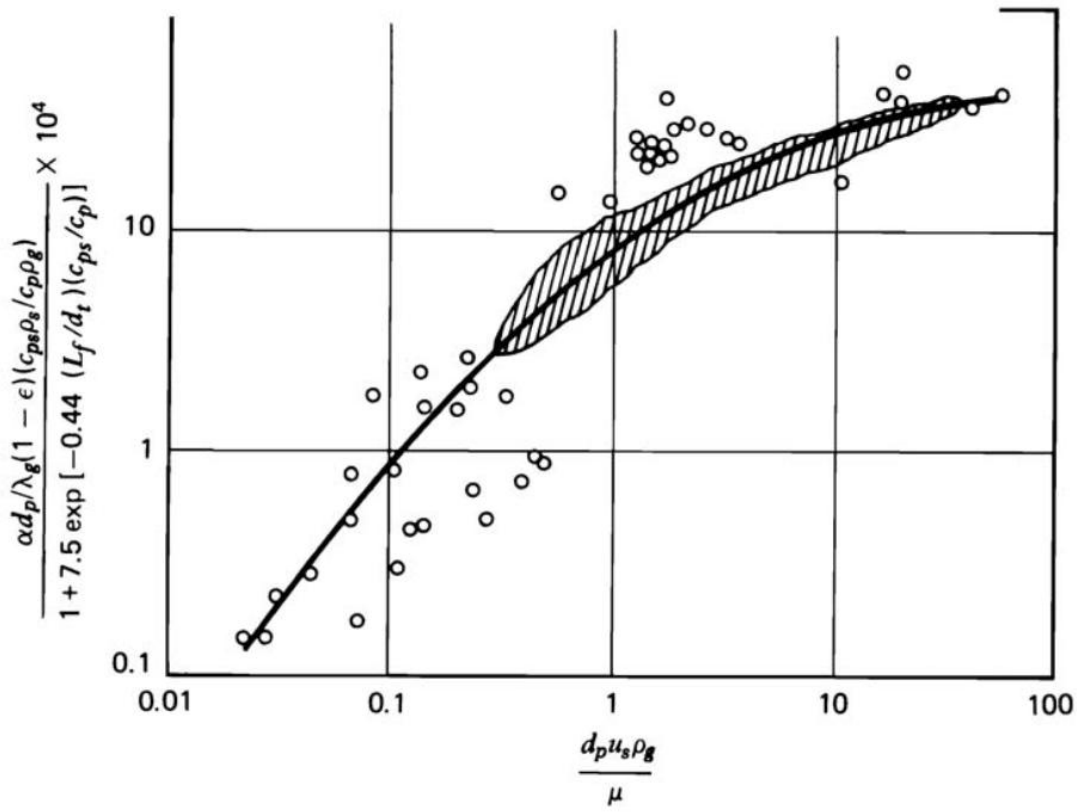


**Figure 5.** Correlation of fluid bed to external surface heat transfer coefficients [Wender and Cooper 1958]. From Zenz and Othmer 1960.

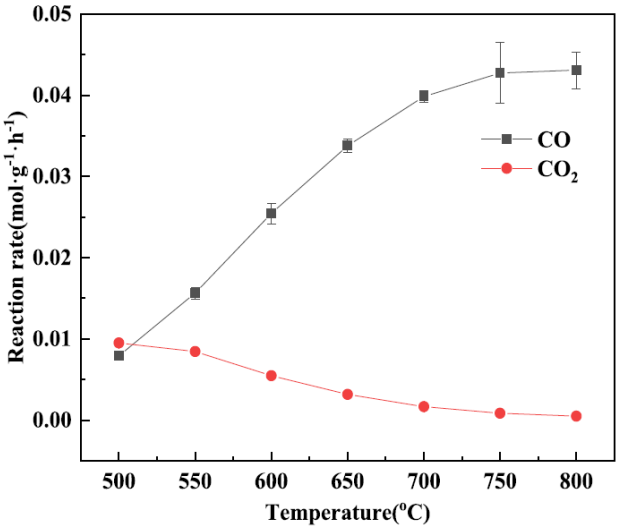


(a)

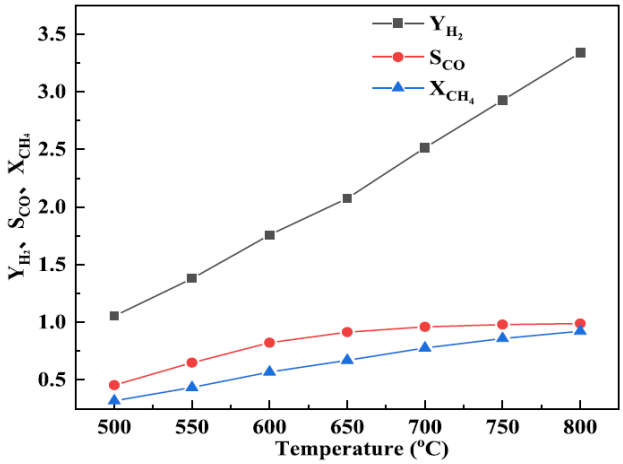


(b)

**Figure 6.** Experimental data of the observed reaction kinetics of Steam Methane Reforming in a Micro-Fluidized Bed used for the Case study [Chen et al., 2020]. (a) Reported observed reaction rates as a function of temperature; (b) $CH_4$ conversion ($X_{CH4}$), CO selectivity ($S_{CO}$), and moles $H_2$ produced per mol $CH_4$ converted ($Y_{H2}$). Figures from the paper of Chen et al. [2020].